

## **Radar Remote Sensing of Agricultural Canopies**

### **A Review**

Steele-Dunne, Susan C.; McNairn, Heather; Monsivais-Huertero, Alejandro; Judge, Jasmeet; Liu, Pang Wei; Papathanassiou, Kostas

**DOI**

[10.1109/JSTARS.2016.2639043](https://doi.org/10.1109/JSTARS.2016.2639043)

**Publication date**

2017

**Document Version**

Accepted author manuscript

**Published in**

IEEE Journal of Selected Topics in Applied Earth Observations and Remote Sensing

**Citation (APA)**

Steele-Dunne, S. C., McNairn, H., Monsivais-Huertero, A., Judge, J., Liu, P. W., & Papathanassiou, K. (2017). Radar Remote Sensing of Agricultural Canopies: A Review. *IEEE Journal of Selected Topics in Applied Earth Observations and Remote Sensing*, 10(5), 2249-2273. Article 7812707. <https://doi.org/10.1109/JSTARS.2016.2639043>

**Important note**

To cite this publication, please use the final published version (if applicable). Please check the document version above.

**Copyright**

Other than for strictly personal use, it is not permitted to download, forward or distribute the text or part of it, without the consent of the author(s) and/or copyright holder(s), unless the work is under an open content license such as Creative Commons.

**Takedown policy**

Please contact us and provide details if you believe this document breaches copyrights. We will remove access to the work immediately and investigate your claim.

# Radar Remote Sensing of Agricultural Canopies: A Review

Susan C. Steele-Dunne, Heather McNairn,

Alejandro Monsivais-Huertero, *Member, IEEE* Jasmeet Judge, *Senior*

*Member, IEEE* Pang-Wei Liu, *Member, IEEE*

and Kostas Papathanassiou, *Fellow, IEEE*,

## Abstract

Observations from spaceborne radar contain considerable information about vegetation dynamics. The ability to extract this information could lead to improved soil moisture retrievals and the increased capacity to monitor vegetation phenology and water stress using radar data. The purpose of this review paper is to provide an overview of the current state of knowledge with respect to backscatter from vegetated (agricultural) landscapes and to identify opportunities and challenges in this domain. Much of our understanding of vegetation backscatter from agricultural canopies stems from SAR studies to perform field-scale classification and monitoring. Hence, SAR applications, theory and applications are considered here too. An overview will be provided of the knowledge generated from ground-based and airborne experimental campaigns which contributed to the development of crop classification, crop monitoring and soil moisture monitoring applications. A description of the current vegetation modelling approaches will be given. A review of current applications of spaceborne radar will be used to illustrate the current state of the art in terms of data utilization. Finally, emerging applications, opportunities and

S. C. Steele-Dunne was with the Department of Water Resources, Faculty of Civil Engineering and Geosciences, Delft University of Technology, Delft, The Netherlands (email: [s.c.steele-dunne@tudelft.nl](mailto:s.c.steele-dunne@tudelft.nl))

H. McNairn is with Agriculture and Agri-Food Canada, Science and Technology Branch, Ottawa, ON K1A 0C6, Canada.

A. Monsivais-Huertero is with the Escuela Superior de Ingeniera Mecnica y Elctrica Ticomn, Instituto Politecnico Nacional, 07738 Mexico City, Mexico.

P.-W. Liu and J. Judge are with the Center for Remote Sensing, Department of Agricultural and Biological Engineering, Institute of Food and Agricultural Sciences, University of Florida, Gainesville, FL 32611 USA.

K. Papathanassiou is with the Information Retrieval Group, Radar Concepts Department, Microwaves and Radar Institute, German Aerospace Center, 82234 Wessling, Germany.

Manuscript received July 8, 2016; revised mmmm dd, yyyy.

20 challenges will be identified and discussed. Improved representation of vegetation phenology and water  
21 dynamics will be identified as essential to improve soil moisture retrievals, crop monitoring and for the  
22 development of emerging drought/water stress applications.

### 23 **Index Terms**

24 IEEE, IEEEtran, journal, L<sup>A</sup>T<sub>E</sub>X, paper, template.

## 25 I. INTRODUCTION

26 Several recent studies suggest that backscatter data, at C-band and higher frequencies, contains  
27 a lot more information on vegetation dynamics than that currently used (e.g. [1]–[3]), with  
28 potential implications for agricultural monitoring. Radar backscatter from a vegetated surfaces  
29 comprises contributions of direct backscatter from the vegetation itself, backscatter from the soil  
30 which is attenuated by the canopy and backscatter due to interactions between the vegetation and  
31 the underlying soil [4]–[6]. The interactions between microwaves and the canopy are influenced  
32 by the properties of the radar system itself, namely the frequency and polarization of the  
33 microwaves, and the incident and azimuth angles at which the canopy is viewed (e.g. [7]–  
34 [10]). Interactions between microwaves and the canopy are governed by the dielectric properties,  
35 size, shape, orientation, and roughness of individual scatterers (i.e. the leaves, stems, fruits etc.)  
36 [11]–[13], [14] and their distribution throughout the canopy [15]–[17]. The dielectric properties  
37 of vegetation materials depend primarily on their water content and to a lesser degree on  
38 temperature and salinity [18], [19]. These crop-specific canopy characteristics vary during the  
39 growing season, and are influenced by environmental conditions and stress [20]–[28]. Scattering  
40 from the underlying soil is influenced by its roughness and dielectric properties (e.g. [29],  
41 [30]), which depend primarily on its moisture content (e.g. [31], [32]). Consequently, there is  
42 significant potential for the use of radar remote sensing in agricultural applications, particularly  
43 classification, crop monitoring and soil/vegetation moisture monitoring. Furthermore, the ability  
44 of low frequency microwaves (1-10GHz) to penetrate cloud cover, and to allow day and night  
45 imaging, ensures timely and reliable observations [33].

46 Currently, most crop classification and crop monitoring activities rely on spaceborne SAR  
47 data due to their finer spatial resolution [34]–[37]. The difficulty in using scatterometry for  
48 crop classification is the mismatch between the resolution requirements for agricultural appli-  
49 cations (from meters in precision agriculture to km for large-scale monitoring) and the spatial

50 resolution attainable with spaceborne scatterometers. These typically have resolutions of tens of  
51 kilometers and are therefore better suited to large-scale vegetation classification and monitoring  
52 [38]–[43]. For soil moisture, on the other hand, both SAR and scatterometry have been used  
53 successfully. High (spatial) resolution SAR observations from ALOS-PALSAR proved sensitive  
54 to soil moisture (e.g. [44]), however the limited revisit time means that they are not suitable  
55 for many applications. NASA’s SMAP mission [45] planned to combine passive radiometry  
56 with SAR measurements, but the radar instrument failed six months after launch in 2015. Soil  
57 moisture observations from ASCAT have been used in a wide range of climate and hydrological  
58 applications [46]–[49]. The archive of ERS1/2 data and the future operational availability of  
59 ASCAT data from MetOp constitutes a soil moisture data cornerstone for climate studies.

60 The goal of this manuscript is to review microwave interactions with vegetation and present a  
61 vision to facilitate the increased exploitation of the past, current and future radar data records for  
62 agricultural applications. A review will be provided of ground-based scatterometer experiments  
63 and airborne radar experiments focussed on crop classification, crop monitoring and soil moisture  
64 retrieval. We will highlight the commonality in how vegetation is modeled for both scatterometry  
65 and SAR applications. It will be shown how this shared heritage contributed to the operational  
66 exploitation of current spaceborne scatterometer and SAR data for crop classification, monitoring  
67 and soil moisture monitoring. We will review recent research indicating that spaceborne radar  
68 observations are sensitive to vegetation dynamics at finer temporal scales than those considered  
69 in current applications. Finally, we will conclude with a vision of how the synergy between  
70 SAR and scatterometry, as well as new ground-based sensors could be utilized to facilitate the  
71 increased exploitation of spaceborne radar observations for agricultural monitoring.

## 72 II. EXPERIMENTAL CAMPAIGNS

73 This section will review the ground-based and aircraft campaigns that contributed to our current  
74 understanding of microwave interactions with vegetation in agricultural landscapes. Tower- and  
75 truck-based scatterometers are used for ground-campaigns, while SAR instruments are more  
76 commonly used in airborne campaigns. Both technologies are used to investigate the sensitivity  
77 of backscatter to soil moisture, and vegetation structure and moisture content as a function of  
78 frequency, polarization and incidence angle. This knowledge has been utilized in the design and  
79 exploitation of spaceborne scatterometry and SAR systems.

## 80 *A. Ground-based scatterometers*

81 Ground-based scatterometers are suitable for the collection of multi-temporal datasets with  
82 high temporal resolution (diurnally, daily or over the entire growth cycle). Data are typically  
83 collected at plot scales. Operating a tower-based instrument is a lot less expensive than flying  
84 an airborne instrument, so the data record can be a lot denser in time than that from an airborne  
85 campaign. It is also much easier to vary the observation parameters such as incidence and azimuth  
86 angle, so it is easy to compare different observation strategies. Detailed and repeated ground data  
87 can be collected at plot scales over time, and plots can be manipulated by imposing specific soil  
88 or crop treatments or by modifying moisture conditions using irrigation. Consequently, ground-  
89 based scatterometer experiments are ideal for collecting the detailed data necessary for theoretical  
90 developments and validation activities and have played a critical component of radar studies for  
91 over forty years.

92 Early field experiments using ground -based scatterometers from the University of Kansas  
93 yielded important preliminary evidence of the sensitivity of radar backscatter to soil moisture and  
94 vegetation cover. The University of Kansas Microwave Active and Passive Spectrometer (MAPS)  
95 from 4-8GHz was used by Ulaby and Moore to demonstrate that sensitivity to soil moisture is  
96 greatest at lower frequencies and in horizontally polarized backscatter and that rain on the soil  
97 makes the surface appear smoother [50]. MAPS was used in one of the first studies to show that  
98 the radar response to soil moisture depends on surface roughness, microwave frequency and look  
99 angle [51]. In a subsequent study in corn, milo, soybeans and alfalfa fields, MAPS was used to  
100 demonstrate that soil moisture could be detected through vegetation cover. They demonstrated  
101 that small incidence angles (5-15 degrees from nadir) and horizontal polarization were best  
102 suited for monitoring soil moisture, while higher frequencies and larger incidence angles were  
103 more sensitive to vegetation and therefore more suited to crop identification/classification [7].  
104 Similar results were also found with the University of Kansas MAS 8-18GHz scatterometer [8].  
105 Measurements of using this system were used for the development and first validation of the  
106 Water Cloud Model [52], discussed in Section III.A. A lower frequency scatterometer, the MAS  
107 1-8GHz, was used to show that frequencies below 6GHz and incidence angles less than 20°  
108 from nadir are best suited to minimize the influence of vegetation attenuation on the relationship  
109 between soil moisture and backscatter. They also showed that row direction has no impact on  
110 cross-polarized backscatter from 1-8GHz, but it does influence co-polarized backscatter below

111 4GHz. Finally, they showed that a linear relationship could be established between soil moisture  
112 and horizontally co-polarized backscatter at 4.25GHz and an incidence angle of 10 degrees. Even  
113 without fitting the data for individual vegetation types, a correlation coefficient as high as 0.80  
114 has been reported. Ulaby et al. [53] showed that for extremely dry soils, the contribution of the  
115 vegetation was very significant but that for the dynamic range of soil moisture of interest in  
116 hydrological and agricultural applications, the influence of vegetation was "secondary" to that of  
117 soil moisture. Data from the MAS 1-8GHz and the MAS 8-18GHz were combined to produce  
118 a clutter model for agricultural crops [54]. Later experiments explored the complexity of the  
119 canopy. Ulaby and Wilson [55] used a truck mounted L-, C- and X-band FMCW scatterometer to  
120 show that agricultural canopies are highly non-uniform and anisotropic at microwave frequencies  
121 resulting in polarization dependent attenuation and soil contribution to backscatter. The relative  
122 contribution of leaves and stalks to total backscatter was also shown to depend on frequency with  
123 leaves accounting for 50% of the canopy loss factor at L-band and 70% at X-band. Tavokoli et  
124 al. used an L-band radar to measure the attenuation and phase shift patterns of horizontally and  
125 vertically polarized waves transmitted through a fully grown corn canopy in order to develop  
126 and evaluate a model for radar interaction with agricultural canopies, explicitly accounting for  
127 the regular plant spacing and row geometry [56].

128 Meanwhile, the Radar Observation of VEgetation (ROVE) experiments in the Netherlands [57]  
129 were focused on the potential of using radar observations in agricultural mapping, monitoring  
130 and yield forecasting. An X-band FMCW scatterometer was mounted on a carriage that could be  
131 moved along fields with a rail system and used to measure at a range of incidence angles from  
132 15 to 80 degrees. This system was used to measure multiple crops, each growing season from  
133 1974 to 1980. Limited airborne observations were also made using a side-looking airborne radar  
134 (SLAR). One of the primary aims was the identification and classification of crops from SLAR  
135 images. Krul [58] used the ROVE data to show that during the growing season, the dynamic  
136 range of X-band backscatter of several crops varied between 3dB and 15dB, underscoring the  
137 importance of accurate calibration. In particular, combining incidence angles was mooted as one  
138 solution to separate the influences of soil moisture and vegetation. Bouman et al. [59] highlighted  
139 the importance of geometry, showing that changes in canopy architecture due to strong winds  
140 could lead to differences of 1-2dB. In sugar beets, the architectural changes in the plants in  
141 the transition from saplings to fully grown plants made it possible to monitor their growth up  
142 to a fractional cover of about 80% and a biomass of 2-3 ton/ha. A thinning experiment, in

143 which some of the plants were removed, suggested that changes in cover due to pest/disease  
144 during the season would be difficult to detect. In barley, wheat and oats, Bouman [60] showed  
145 that the interannual variability in backscatter could be as much as the range due to growth.  
146 Nonetheless, X-band backscatter could be useful for the classification and detection of some,  
147 though not all, developmental phases. In particular, soil moisture variations confounded the  
148 detection of emergence and harvest. Bouman [61] suggested that multi-frequency observations  
149 might be useful to separate the backscatter contributions from potato, barley and wheat thereby  
150 improving the estimation of dry canopy biomass, canopy water content, fractional cover, and  
151 crop height.

152 Ground-based scatterometer experiments have been used extensively, especially in early SAR  
153 research, to gain an understanding of responses as targets change and SAR configurations are  
154 modified. They allowed scientists to develop and test methodologies prior to the engineering of  
155 SAR satellite systems, and before space-based data became available. In addition to collecting  
156 data for model development and testing, scatterometers can also be used in novel ways to study  
157 phenomenon not easily implemented using air- or space-borne systems. Inoue et al [62] used a  
158 multi-frequency polarimetric scatterometer to measure backscatter over a rice field once per day  
159 for an entire growing season in order to relate the microwave backscatter signature to rice canopy  
160 growth variables. They investigated the influence of rice growth cycle on backscatter at L-, C-,  
161 X-, Ku- and Ka- bands for a range of incident and azimuth angles and their relationship to LAI,  
162 stem density, crop height and fresh biomass. The Canada Centre for Remote Sensing (CCRS)  
163 acquired a ground-based scatterometer in 1985 which was dedicated primarily to agriculture  
164 research. This was a 3-band system mounted on a hydraulic boom supported on the flat bed  
165 of a 5-ton truck. The scatterometer acquired data at L, C and Ku bands (1.5 GHz, 5.2 GHz,  
166 12.8 GHz) and at four polarizations: HH, VV, HV, VH. The boom allowed a change in incident  
167 angle, with operations typically at 20 to 50°.

168 Some of the earliest research using the CCRS scatterometer looked at crop separability. Brisco  
169 et al. [63] reported the best configurations for this purpose, i.e. higher frequencies (Ku-band as  
170 opposed to C- or L-bands), the cross polarization, shallower incident angles and observations  
171 during crop seed development. These conclusions have been reinforced by many subsequent  
172 studies, whether using airborne or satellite based SAR observations. The diurnal effects of  
173 backscatter were tracked by Brisco et al. [64]. Backscatter was sensitive to daily movement of  
174 water, mostly due to the diurnal pattern of water in plants during active growth, and due to the

175 diurnal pattern of soil moisture during periods of crop senescence. Toure et al. [65] modified the  
176 MIMICS model to accommodate agricultural parameters and used the scatterometer to validate  
177 the accuracy of this modified model to estimate soil moisture as well as stem heights and leaf  
178 diameters.

179 Investigations into the sensitivity of backscatter to soil moisture, crop residue and tillage were  
180 a focus of a number of scatterometer investigations. Major et al. [66] found that backscatter was  
181 sensitive to soil moisture even in the presence of a short-grass prairie conditions. Meanwhile  
182 Boisvert et al. [67] modelled the effective penetration depth for L-, C-, and Ku-bands, an im-  
183 portant consideration in validation of soil moisture retrievals even with current satellite systems.  
184 Data from the scatterometer allowed Boisvert et al. [67] to forward model soil moisture for  
185 various models (Oh, Dubois and the IEM) and to evaluate the performance of these models  
186 against field data. Assessment of model approaches was also a focus of scatterometer research,  
187 with McNairn et al. [68] using a dual incident angle approach to estimate both soil moisture  
188 and roughness.

189 Canadian researchers also imposed tillage and residue treatments on field plots, irrigating  
190 these plots to simulate various wetness conditions. These studies confirmed that residue is not  
191 transparent to microwaves when sufficiently wet, and that in fact cross polarizations can be very  
192 sensitive to the amount of residue present [69], [70]. Airborne and satellite data often detect  
193 "bow-tie" effects on agricultural fields due to tillage, planting and harvesting direction. This  
194 was also reported by Brisco et al. [71] but this study was one of the first to reveal that the  
195 cross-polarization is much less affected by look direction. This is an important consideration  
196 for agriculture given that significant errors in soil moisture retrievals can be introduced by this  
197 effect [67].

198 The development of a retrieval algorithm for NASA's SMAP mission spurred several ground-  
199 based radar experiments [72]. NASA's ComRAD system is an truck-based SMAP simulator  
200 that includes a dual-pol 1.4GHz radiometer and a 1.24-1.34GHz radar [73]. The instrument is  
201 mounted on a 19m hydraulic boom and is typically configured to measure at a 40° incidence  
202 angle similar to that of SMAP, though it can sweep in both azimuth and incidence angle. Early  
203 deployments focussed on forest attenuation of the soil moisture signal ( [74], [75]). O'Neill et al.  
204 [76] collected active and passive L-band observations over a full growing season in adjacent corn  
205 and soybean fields to refine the SMAP retrieval algorithms. In particular, these data yield insight  
206 into the influence of changing vegetation conditions and the relationship between contempora-

207 neous active and passive observations. Svirastava et al. [77] used this data to compare different  
208 approaches to estimate vegetation water content (VWC). The combined active/passive ComRAD  
209 system meant that they could compare backscatter in different polarizations, polarization ratios,  
210 Radar Vegetation Index (RVI) and Microwave Polarization Difference Index (MPDI). They found  
211 that at L-band, HV backscatter was the best estimator for vegetation water content (VWC). This  
212 is a valuable result as it obviates the need for ancillary data, like NDVI and a parameterization  
213 to provide VWC for the retrieval algorithm.

214 The University of Florida L-band Automated Radar System (UF-LARS) [78] operates at  
215 1.25 GHz and can be used to observe VV, HH, HV, and VH backscatter every 15 minutes for  
216 several weeks. Measurements are typically made from a height of about 16 m above the ground  
217 with an incidence angle of 40°. The ability of UF-LARS to measure with such high temporal  
218 resolution and over long periods offers a unique insight into the backscatter signature of near-  
219 surface soil moisture dynamics in response to precipitation, irrigation and other environmental  
220 conditions. The density and accuracy of data also renders it ideal for developing and validating  
221 backscattering models. The UF-LARS has been used to investigate the dominant backscattering  
222 mechanisms from bare sandy soils, to evaluate the sensitivity of backscatter to volumetric soil  
223 moisture [79] and growing vegetation [78], to investigate the benefit of combining active and  
224 passive microwave observations for soil moisture estimation [80] and to evaluate uncertainty  
225 in the SMAP downscaling algorithm for sweet corn [81]. Data from UF-LARS were used by  
226 Monsivais-Huertero et al. to compare bias correction approaches used in the assimilation of  
227 active/passive microwave observations to estimate soil moisture [82].

228 Finally, the Hongik Polarimetric Scatterometer (HPS) is a quad-pol L-, C- and X-band scat-  
229 terometer that operates on a tower [83]. It has been used for model development and cross-  
230 comparisons with satellite data over a number of crops [84]–[86], and to develop a modified  
231 form of the Water Cloud Model in which the leaf size distribution is parameterized [87]. Inclusion  
232 of an additional antenna and modifications to the mechanical system also allow it to be configured  
233 as a rotational SAR system [88]

### 234 *B. Airborne radar instruments*

235 One drawback of ground-based investigations is the rapid change of the imaging geometry in  
236 range and cross-range across a relatively small scene. Near-field effects (i.e. the curved wavefront  
237 interacting with tall crops) also need to be taken into account. The main limitation of using

238 ground-based scatterometers is that they measure a single field or, at best, can be moved with  
239 a mechanical system to observe multiple fields. This greatly limits the diversity of fields and  
240 conditions that can be observed in a single campaign. Aircraft-mounted sensors allow measure-  
241 ments along flight lines spanning many fields which may include different crops, roughness  
242 characteristics, growth stages and moisture content. However, an aircraft campaign is typically  
243 limited to a few flights. Airborne radar instruments therefore offer a complementary perspective  
244 to that from tower-based instruments. In Europe, the 1-18GHz DUT SCATterometer (DUTSCAT)  
245 [89] and the C-/X-band ERASME helicopter-borne scatterometer [90] were deployed over five  
246 test sites during the AGRISCATT88 campaigns that built on the knowledge and expertise gained  
247 from the ROVE experiments [91]. Bouman et al. [92] used the DUTSCAT data to investigate  
248 the potential of multi-frequency radar for crop monitoring and soil moisture. Their analysis  
249 confirmed findings from their earlier ground-based study [61] that the sensitivity of backscatter  
250 to canopy structure complicates the retrieval of biomass, soil cover, LAI and crop height. They  
251 also confirmed that higher frequencies (X- to K-band) were best suited to crop separability,  
252 while L-band yielded the most information on soil moisture in bare soils. Similar conclusions  
253 were drawn by Ferrazzoli et al. [93] from an analysis of the DUTSCAT and ERASME datasets.  
254 They used the same datasets to demonstrate that leaf dimensions had a significant influence on  
255 backscatter from agricultural canopies, particularly at S- and C-band [94]. Schoups et al. [95]  
256 used the DUTSCAT data to investigate the sensitivity of backscatter from a sugar beet field to  
257 soil moisture and roughness, leaf angle distribution and moisture content, canopy height, and  
258 incidence angle and frequency. Prevot et al [96] used the ERASME data to develop a modified  
259 version of the Water Cloud Model in which multi-angle data is used to account for roughness  
260 effects, and presented an inversion approach capable of retrieving vegetation water content where  
261 LAI is less than 3. Benallegue et al. [97] analyzed the ERASME data collected over the Orgeval  
262 basin (France) to evaluate the use of multi-frequency, multi-incidence angle radar observations for  
263 soil moisture retrieval. Their results were consistent with early results of Ulaby et al. in that low  
264 frequency (C-band in this case) observations 20° from nadir contained most information on soil  
265 moisture while the higher frequency (X-band) observations at larger incidence angles were used  
266 to quantify the vegetation attenuation. Benallegue et al. [98] subsequently used the ERASME data  
267 to argue that variability in soil dielectric constant (moisture content) and roughness precludes  
268 the use of SAR (e.g. ERS-1 SAR) to estimate soil moisture at a single field level, but that  
269 larger scale trends in the basin could be detected if the measurements were on a scale of about

270 1km. These early airborne experiments demonstrated the robustness of the theories and models  
271 developed from ground-based scatterometry over larger areas and for a wider range of land  
272 cover and crop types. The international community involved in collecting both airborne data and  
273 ground data is indicative of the growing interest in using radar for crop classification and crop  
274 and soil monitoring at that time.

275 In the 1980s the Canadian CV-580 SAR was developed as a multi-frequency (L-, C- and  
276 X-band) airborne system. The CV-580 was flown in support of many early agricultural experi-  
277 ments, demonstrating the value of SAR for crop classification, whether by integrating SAR with  
278 optical data [99] or simply using its multiple frequency capability [100]. Later the system was  
279 modified to incorporate full polarimetry on C-band [101]. This mode was instrumental for the  
280 scientific community, providing data to develop polarimetric applications in advance of access  
281 to such data from satellites systems. These airborne data led to many early discoveries regarding  
282 the value of polarimetry. McNairn et al. [102] used these data to investigate polarization for  
283 crop classification, discovering that three C-band polarizations (whether linear or circular) were  
284 sufficient to accurately classify crops. In fact the best 3-polarization combination included the  
285 LL circular polarization (HH-HV-LL). Data collected by the airborne CV-580 also assessed the  
286 value of polarimetry for crop condition assessment. McNairn et al. [103] used several linear  
287 polarizations at orientation angles of  $45^\circ$  and  $135^\circ$  and circular (RR and RL) polarizations to  
288 classify fields of wheat, canola and peas into productivity zones, indicative of variations in crop  
289 height and density. C-band polarimetric data from the CV-580 also demonstrated that linear and  
290 circular polarizations could classify wheat fields into zones of productivity weeks before harvest  
291 [104]. These zones were well correlated with zones defined by yield monitor data.

292 The CV-580 was instrumental in efforts to ready the international community to exploit data  
293 from Canada's first satellite, RADARSAT-1. The GlobeSAR-1 program was initiated in 1993, two  
294 years prior to the launch of RADARSAT-1, with objectives to acquaint users with the application  
295 of this new data source and to facilitate use of imagery from the ERS-1 satellite [105]. The  
296 CV-580 travelled approximately 100,000 km, acquiring more than 125,000  $km^2$  of multi-mode  
297 SAR data over 30 sites in twelve countries including France, the UK, Taiwan, China, Vietnam,  
298 Thailand, Malaysia, Kenya, Uganda, Jordan, Tunisia and Morocco [106]. C- and X-band multiple  
299 polarization as well as fully polarimetric data from this campaign fuelled early research into a  
300 diversity of applications including rice identification and monitoring, soil moisture estimation  
301 and land cover mapping [107]. In China, these data were used to develop multi-polarization and

302 multi-frequency based land cover maps with accuracies close to 90%; in Thailand CV-580 data  
303 were combined with TM and SPOT data to improve land cover discrimination. The data collected  
304 by this airborne platform and the SAR training delivered during the GlobeSAR-1 program had  
305 a lasting impact for RADARSAT applications in these regions.

306 By the late 1990s, its high resolution capabilities meant that SAR had been identified as the  
307 way forward in terms of crop classification and monitoring. Several airborne campaigns using  
308 Experimental-SAR (E-SAR) system from the German Aerospace Center (DLR) were conducted  
309 in Europe to prepare for the availability of spaceborne radar data from Sentinel-1 and TerraSAR-  
310 X. During the TerraSAR-SIM campaign (Barrax, Spain in 2003), DLR's airborne E-SAR system  
311 was used during five flights to quantify the impact of time lag between satellite acquisitions at  
312 different wavelengths on agricultural applications, particularly classification and crop monitoring  
313 [108]. The data collected were used again recently to test retrievals of above ground biomass in a  
314 wheat canopy using CosmoSky-Med and Sentinel-1 SAR data [109]. The Bacchus campaign and  
315 follow-up activities also employed DLR's E-SAR system to evaluate the potential for using C-  
316 and L-band SAR in viticulture [110]. In addition to gaining insight into the scattering mechanisms  
317 in vineyards [111], the synergy of combining radar and optical imagery for classification purposes  
318 was considered [112]. E-SAR was also combined with spectral data during the AQUIFEREx  
319 campaign to produce high-resolution land maps for water resources management in Tunisia  
320 [113]. During the Eagle2006 campaign ([114]), L-, C- and X-band data were acquired over  
321 three sites in the Netherlands. C-band images were used to simulate Sentinel-1 data, to facilitate  
322 the development and testing of retrieval algorithms. Optical and thermal imagery, as well as  
323 extensive ground measurements were also collected over grass and forest sites. E-SAR was also  
324 flown during the AgriSAR2006 campaign during which in-situ data, and satellite imagery were  
325 combined with airborne SAR and optical imagery to support decisions regarding the instrument  
326 configurations for the first Sentinel Missions [115], [116]. The data were used to investigate  
327 the impact of polarization on crop classification [37], to develop algorithms for soil moisture  
328 retrieval from SAR [10], [117], [118].

329 In preparation for NASA's Soil Moisture Active Passive (SMAP) mission, NASA's Jet Propul-  
330 sion Laboratory developed the Passive Active L- and S-band System (PALS) instrument to  
331 investigate the benefit of combining passive and active observations. It has been deployed  
332 during several experiments in the last two decades [119], [120]. Earlier experiments such as  
333 measurements conducted in the Little Washita Watershed, OK, during Southern Great Plains

334 experiment 1999 (SGP99), and in the Walnut Creek, IA, during Soil Moisture Experiment 2002  
335 (SMEX02) were primarily to understand the sensitivities of the multi-frequency and -polarized  
336 active and passive observations. Although the studies found great sensitivities of both active  
337 and passive observations to the soil moisture, the active observations were more sensitive to  
338 the variation of vegetation conditions [121], [122]. In agreement with the earliest ground-based  
339 experiments, the L-band observations were more sensitive to the soil moisture changes due to  
340 better penetration in the agricultural region, while those from the S-band were more sensitive  
341 the vegetation water content.

342 PALS still plays a significant role in NASA-SMAP pre- and post-launch calibration and  
343 validation activities through the so-called SMAP Validation Experiments (SMAPVEX) [123],  
344 [124]. Airborne PALS data been used to test and modify soil moisture retrieval algorithms  
345 in agricultural regions [120], [124], and to develop downscaling algorithms for high spatial  
346 resolution soil moisture under different levels of vegetation water content by integrating the active  
347 and passive observations for SMAP [125], [126]. Similar to PALS, an airborne Polarimetric L-  
348 band Imaging SAR (PLIS) was designed and combined with the Polarimetric L-band Multibeam  
349 Radiometer (PLMR) to support the development of soil moisture algorithms for the SMAP  
350 mission in Australia [127]–[129]. Five field campaigns, called SMAP Experiments (SMAPExs),  
351 have been conducted using PLIS from 2010-2015 in agricultural and forest regions in south-  
352 eastern Australia. Wu et al. [130], [131] used the observations from SMAPEx1-3 to validate  
353 and calibrate the SMAP simulator and to evaluate the feasibility and uncertainty of the SMAP  
354 baseline downscaling algorithms.

### 355 III. ACCOUNTING FOR BACKSCATTER FROM VEGETATION

356 Data collected in the experimental campaigns discussed in the previous section have been  
357 used to develop, test and validate models to simulate the influence of the soil and vegetation  
358 on backscatter. In this section, the most common ways in which backscatter from a vegetated  
359 surface is simulated/interpreted are reviewed. The Water Cloud Model, and Energy and Wave  
360 approaches are used for both forward modeling and inversion to obtain soil moisture, vegetation  
361 water content or biomass and/or Leaf Area Index. SAR decompositions quantify the contributions  
362 of surface, volume and double-bounce backscatter to the total power and are particularly useful  
363 for classification and growth stage identification.

364 For vegetated terrain, the effects of canopy constituents, geometry, and moisture distribution  
 365 are typically modeled as a scattering phase function, extinction coefficient, and scattering albedo,  
 366 as described by Ulaby et al. [132]. The canopy can be modeled either as a continuous media  
 367 with statistical dielectric variations within the canopy or as a discrete layered medium [133].

### 368 *A. The Water Cloud Model*

369 In 1978, Attema and Ulaby published the Water Cloud Model (WCM), an approach to  
 370 characterize a vegetation canopy as a collection of uniformly distributed water droplets [132].  
 371 The WCM is a zeroth-order radiative transfer solution in which the power backscattered by  
 372 the entire canopy is modeled as the incoherent sum of the contributions from the canopy (as  
 373 a whole) as well as the underlying soil. In this model, multiple scattering (between soil-canopy  
 374 and within the canopy) is ignored [52]. [96]. The canopy can be represented with one or two  
 375 vegetation parameters. The WCM has been adapted to model scattering from a range of crop  
 376 canopies. Prevot et al. [96] review these approaches, which have considered canopy (or leaf)  
 377 water content and Leaf Area Index (LAI) as descriptors of the vegetation canopy. In the WCM,  
 378 total backscatter  $\sigma^0$  is modeled according to incoherent scattering from vegetation  $\sigma_{veg}^0$  and  $\sigma_{soil}^0$ .  
 379 Two-way transmission-backscatter through the canopy attenuates the signal and is modeled using  
 380 an attenuation factor  $\tau^2$ :

$$\sigma^0 = \sigma_{veg}^0 + \tau^2 \sigma_{soil}^0 \quad (1)$$

$$\sigma_{veg}^0 = AV_1 \cos \theta (1 - \exp(-2BV_2 / \cos \theta)) \quad (2)$$

$$\tau^2 = \exp(-2BV_2 / \cos \theta) \quad (3)$$

381 where A and B are the parameters of the model and  $\theta$  is the incidence angle.  $V_1$  and  $V_2$  are  
 382 canopy descriptors. One vegetation parameter can be used for both  $V_1$  and  $V_2$ , or alternatively  
 383 different parameters can be assigned to each of  $V_1$  and  $V_2$ . Direct scattering from the soil must  
 384 be modeled within the WCM. Typically, a simple linear model has been used as Ulaby et al.  
 385 (1978) demonstrated that scattering from the soil can be expressed as a simple linear function  
 386 between backscatter and soil moisture,  $M_v$ :

$$\sigma_{soil}^0 = CM_v + D \quad (4)$$

387 where C and D are the slope and intercept of the relationship between backscatter and soil  
 388 moisture. Some attempt has been made to use more physically based approaches to model

389 scattering from the soil, including integration of the physically-based Integral Equation Model  
390 (IEM) with the WCM [134].

391 The attraction of the WCM is that this is a relatively simple model whereby given a sufficient  
392 number of radar measurements (in multiple angles, polarizations and/or frequencies), both the  
393 vegetation canopy parameters and soil moisture can be simultaneously estimated. However, the  
394 WCM is a semi-empirical model whereby parameterization of the vegetation and soil variables  
395 is accomplished using experimental data. As such, performance of the model is affected by the  
396 quality and robustness of these data. The WCM has typically been parameterized on a crop-  
397 specific basis given that the vegetation structure varies significantly among different species. If  
398 multiple radar measurements are used, inversion of the WCM allows estimates of vegetation  
399 parameter(s), for example LAI and/or vegetation water content, as well as underlying soil  
400 moisture [96], [135], [136]. Alternatively, soil moisture data can be supplied to estimate the  
401 vegetation parameters [137], or vegetation data can be provided to estimate the soil moisture  
402 [138].

403 The simplicity of the WCM means that it is easy to parameterize and use for forward modeling  
404 and retrieval. However, its assumption regarding the uniform distribution of moisture in the  
405 canopy is a huge simplification of reality. Figure 1 illustrates the dynamics of the vertical moisture  
406 content distribution in corn during a growing season from destructive data collected in the  
407 Netherlands in 2013. Figure 1(a) shows the vegetation leaf water content in  $kgm^{-2}$ . Each dot  
408 corresponds to the total VWC of leaves at a certain height (indicated on the y-axis), in one square  
409 meter. Figure 1(b) shows the water content of the stems in  $kgm^{-2}$ . Each dot corresponds to the  
410 total water content in all stems in the 10cm stems centered at that height (indicated on the y-axis),  
411 in one square meter. Figure 1(a) and (b) demonstrate that, in contrast to the assumption of the  
412 WCM, the moisture in the canopy is far from evenly distributed. Most of the water stored as leaf  
413 water is concentrated in the mid-section where the largest leaves occur. During the vegetative  
414 stages (up to 27 July), the moisture distribution in the stem is relatively uniform, decreasing  
415 only slightly with height. When the ears start to form and separate from the stem, the stem  
416 VWC at and above the ears becomes relatively dry. The gradient in stem VWC as a function  
417 of height becomes clearer and it changes as the season progresses. The contributions of leaf,  
418 stem and ear moisture to the total is shown in Figure 1 (c). This illustrates that the distribution  
419 of canopy water content among the different scatterers also varies during the growing season.  
420 The influence this has on backscatter depends on frequency and polarization. It is clear that the

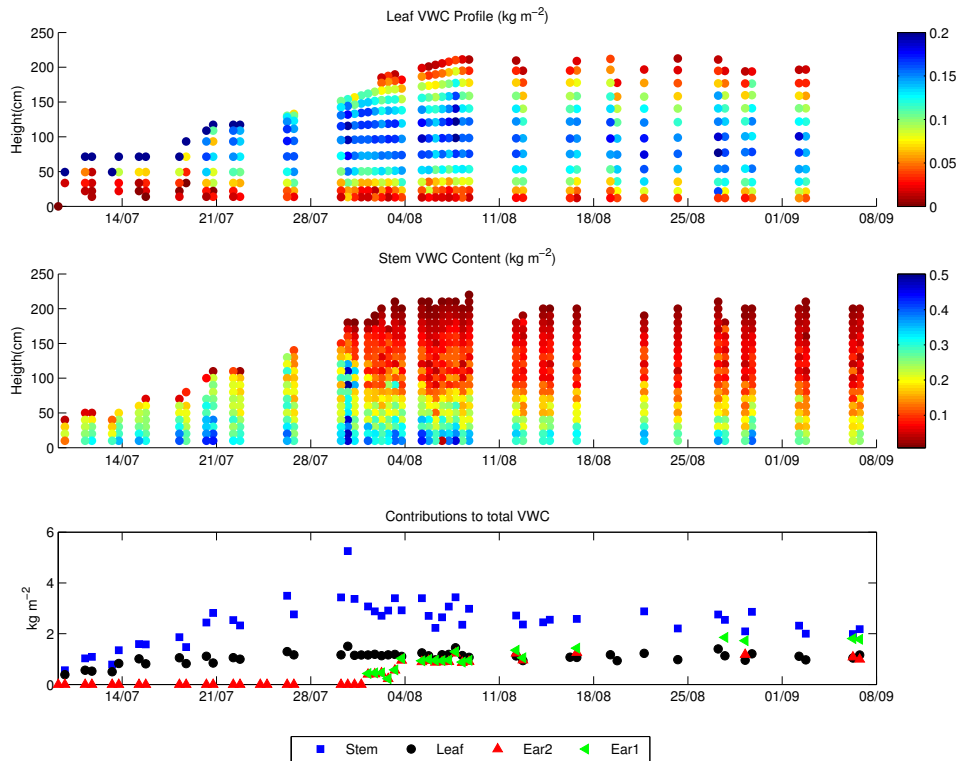


Fig. 1. Vertical distribution of leaf (a) and stem (b) moisture content, and the contributions of leaf, stems and ears to total Vegetation Water Content ( $kgm^2$ )(c) in an unstressed corn canopy.

421 assumptions of the WCM are very simplistic compared to the actual distribution and dynamics  
 422 of water content during the growing season.

423 *B. Energy and Wave approaches*

424 Equation 1 can be formulated as

$$\sigma^0 = \sigma_{soil}^0 + \sigma_{veg}^0 + \sigma_{sv}^0 \quad (5)$$

425 so that the total backscatter from the vegetated surface  $\sigma^0$  includes scattering contributions from  
 426 the soil surface ( $\sigma_{soil}^0$ ), direct scattering from the vegetation ( $\sigma_{veg}^0$ ), and from interactions between  
 427 soil and vegetation ( $\sigma_{sv}^0$ ) [4]. The  $\sigma_{soil}^0$  is a function of the reflectivity of the soil and is highly  
 428 sensitive to surface roughness. The  $\sigma_{veg}^0$  is a function of canopy opacity and geometry. For a  
 429 mature crop,  $\sigma_{veg}^0$  could comprise a significant portion of  $\sigma^0$  [139].

430 Scatterers within the layered medium are characterized by canonical geometric shapes such  
431 as ellipsoids or discs for leaves and cylinders for trunks, branches, and stems [17]. Typically,  
432 the vegetation consists of a canopy layer within which these objects are randomly arranged, a  
433 stem layer with randomly located nearly vertical cylinders that may or may not extend into the  
434 branch layer, if present, and an underlying rough ground. Several backscattering models exist  
435 for vegetated terrain, e.g. [140]–[143]. The  $\sigma^0$  for the vegetated terrain can be estimated either  
436 through the energy or intensity approach or the wave approach [144].

437 Both the energy and the wave approaches are based on physical interactions of electromagnetic  
438 waves with vegetation. In the energy approach, only amplitudes of the electromagnetic fields  
439 are estimated. The backscattering is described either through radiative transfer (RT) equations  
440 [145], Matrix Doubling theory [146], or Monte Carlo simulations [147]. The RT models (e.g.  
441 Michigan Microwave Canopy Scattering (MIMICS), [143] and the Tor-Vergata Model [148]) are  
442 energy-based equations that govern the transmission of energy through the scattering medium.  
443 According to the radiative transfer theory, the propagating energy interacts with the medium  
444 through extinction and emission. Extinction causes a decrease in energy, while emission accounts  
445 for the scattering by the medium along the propagation path. For a medium with random particles,  
446 the RT theory assumes that the waves scattered from the particles are random in phase and the  
447 total scattering can be estimated by incoherent summation over all particles. Thus, the extinction  
448 and emission processes can be represented by the average extinction and source matrices within  
449 each layer. The RT models represent a first-order solution and use Foldy's approximation to  
450 estimate a mean field as a function of height within the vegetation. This mean field is then  
451 scattered from each of the vegetation constituents. Soil surface scattering and specular reflection  
452 are denoted by scattering and reflectivity matrices. The intensities across interfaces are continuous  
453 under the assumption of a diffuse boundary condition.

454 The MIMICS model represents the vegetation as divided in three regions: the crown region, the  
455 trunk region, and the underlying ground region [133]. The Radiative Transfer equations are solved  
456 iteratively in a two-equation system; one represents the intensity vector into upward direction  
457 and the second equation represents the intensity into the downward direction. The Tor Vergata  
458 model divides the vegetation into  $N$  layers over a dielectric rough surface. Each layer is described  
459 by the upper half-space intensity scattering matrix and the lower half space intensity scattering  
460 matrix. To compute the total scattered field from the scene, the matrix doubling algorithm is  
461 used, under the assumption of azimuthal symmetry. The first-order solution of both RT models

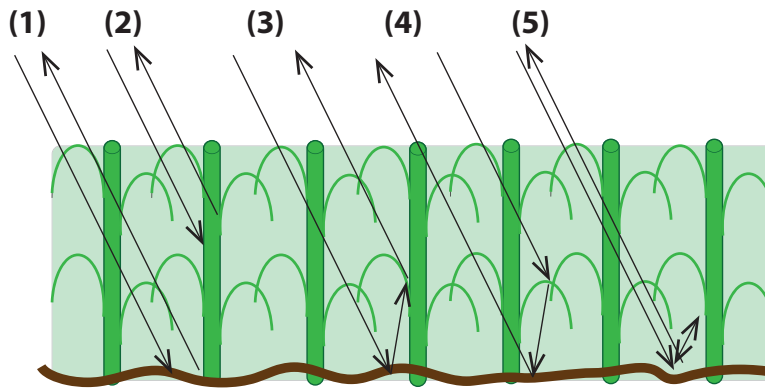


Fig. 2. Scattering mechanisms considered in the first-order models for both energy and wave based approaches: (1) direct ground (2) direct vegetation (3) ground-vegetation (4) vegetation-ground (5) ground-vegetation-ground

462 accounts for five scattering mechanisms, as shown in Figure 2 (1) direct scattering from soil  
 463 ( $\sigma_{soil}^0$ ), (2) direct scattering from vegetation ( $\sigma_{veg}^0$ ); (3) ground reflection followed by vegetation  
 464 specular scattering, (4) vegetation specular followed by ground reflection; and (5) double bounce  
 465 by ground reflection and/or vegetation backscattering and ground reflection. The addition of the  
 466 scattering mechanisms 3, 4 and 5 are represented by  $\sigma_{sv}^0$  in Equation 5.

467 Though MIMICS was originally developed for forest canopies [143], [65] modified it for use  
 468 in agricultural (wheat and canola) canopies by removing the distinct trunk layer, expressing the  
 469 constituents of canola and wheat in terms of cylinders, discs and rectangles, and parameterizing  
 470 leaf density as a function of input LAI. A similar approach was employed by Monsivais-Huertero  
 471 and Judge [139] to model a maize canopy. DeRoo et al. [149] adapted the MIMICS to model the  
 472 soybean crop and Liu et al. [150] used MIMICS to assimilate the backscattering coefficient into  
 473 a soybean growth model. The Tor-Vergata model has been used to test classification schemes  
 474 [151], the evaluate the potential of radar configurations for applications [152], [153] and to yield  
 475 insight into radar sensitivity to crop growth [154]–[156].

476 In the wave approach, both the phase and amplitude of the electromagnetic fields are computed  
 477 and Maxwell's equations are used to derive the bistatic scattering coefficient. The mean field in  
 478 the medium can be calculated using the Born approximation (neglects multiple scattering effects)  
 479 and the renormalization bilocal approximation (accounts for both absorption and scattering).  
 480 Similar to the energy approach, the models based upon the wave approach (e.g. [157]–[161])  
 481 consider horizontally-layered random vegetation and the five scattering mechanisms represented  
 482 in Figure 2. Unlike the energy approach, the wave approach adds, in amplitude and phase, the

483 scattered field by each vegetation constituent (branches, stems, leaves, etc.), accounting for the  
484 orientation and relative position of the constituents. The attenuation and phase shifts within the  
485 vegetation are calculated using Foldy's approximation. The total  $\sigma^0$  is obtained by averaging  
486 several realizations of randomly generated vegetation.

487 Several studies have compared the two approaches. Chauhan et al. [162] found  $\sigma^0$  higher by  
488 3dB when ground-vegetation-ground interaction was considered for estimating backscatter from  
489 corn in mid season at L-band compared to the case when the interaction was ignored. Including  
490 the coherent effects produced  $\sigma^0$  estimates that were closer to observations. Recently, Monsivais-  
491 Huertero and Judge [139] found similar differences between the two approaches during the  
492 entire growing season of corn, from bare soil to maturity, at L-band. The coherent effects had a  
493 particularly high impact during the reproductive stage of the corn, due to the ears. When each term  
494 in Equation (1) was examined closely, it was found that the RT approach predicted  $\sigma_{veg}^0$  as the  
495 primary contribution, while the wave approach predicted  $\sigma_{sv}^0$  as the dominant contribution. The  
496 HH polarization showed higher differences between the two approaches than the VV polarization,  
497 suggesting that the HH polarization is more sensitive to the coherent effects for a corn canopy.  
498 The study also indicated that ears were the main contributors during the reproductive stage.  
499 Coherent effects were also found to be significant when Stiles and Sarabandi [159], [160] found  
500 that the row periodicity of agricultural field had an impact in the azimuth look angle, particularly  
501 at low frequencies such as the L-band.

502 Energy and Wave approaches require moisture content or dielectric properties of the soil and  
503 vegetation as well as a description of the size, shape, orientation and distribution of scatterers  
504 in the canopy. This limits their usefulness to the wider, non-expert community. Despite their  
505 complexity, it is important to note that the representing vegetation as a collection of ellipsoids,  
506 discs etc., is still a crude simplification of reality. It remains unclear whether such a description is  
507 better than more simple, physical models. Nonetheless, they are very useful for relating ground  
508 measurements of the parameters during field campaigns to ground-based, airborne or satellite-  
509 based observations and interpreting their respective contributions to backscatter.

### 510 *C. Polarimetric Decompositions*

511 Polarimetric radar decomposition methods separate total scattering from a target into elemen-  
512 tary scattering contributions. This technique can be helpful for establishing vegetation health and  
513 for classifying land cover as the dominance and strength of surface (single-bounce), multiple

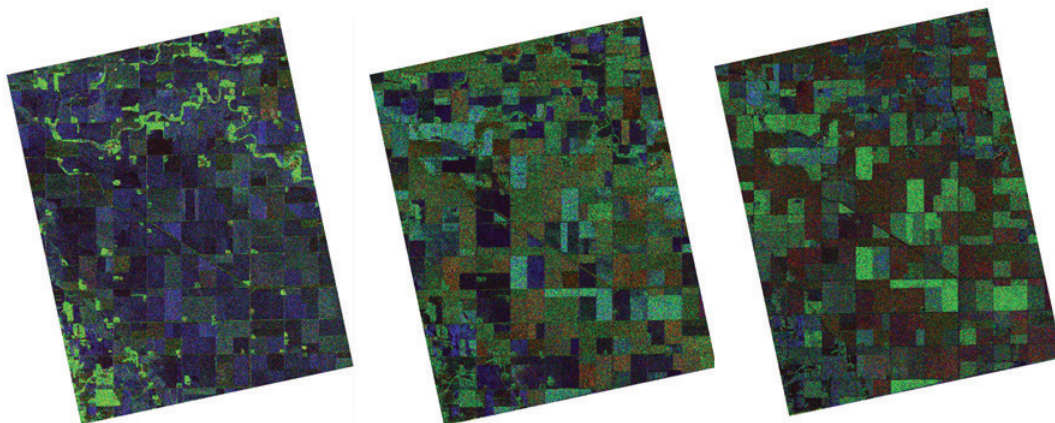


Fig. 3. Freeman-Durden decomposition of RADARSAT-2 quad-polarization data from the 2012 SMAPVEX experiment in Manitoba (Canada). The left image is from April 26, middle from June 13 and right from July 7. Surface scattering is displayed in blue, volume scattering in green and double bounce in red.

514 (volume) and double-bounce scattering is largely driven by the roughness and/or structure of the  
 515 target. More specifically the structure of vegetation varies by type, condition and phenology state,  
 516 and as these vegetation states vary so does the mixture and strength of scattering mechanisms.  
 517 Different polarimetric decomposition approaches allow the polarimetric covariance matrix to be  
 518 decomposed into contributions assigned to single or odd bounce scattering (indicative of a direct  
 519 scattering event with the vegetation or ground), double or even bounce scattering (indicative of a  
 520 scattering event between, for example, a vegetation stalk and the ground) and volume scattering  
 521 (indicative of multiple scattering events between the ground and vegetation, or among vegetation  
 522 components) [163], [164]. Yamaguchi [165] added a fourth scattering component (helix scattering)  
 523 to account for co-polarization and cross-polarization correlations, as some contributions from  
 524 double bounce and surface scattering were thought to be contributing to volume scattering [166],  
 525 [167].

526 Figure 3 shows the Freeman-Durden decomposition of three RADARSAT-2 quad-polarization  
 527 images obtained during SMAPVEX 2012 in Manitoba (Canada). The cropping mix in this region  
 528 is dominated by spring wheat, canola, corn and soybeans. In April, producers have yet to plant

529 their crops for the season, so surface and volume scattering from bare soil dominate. In the July  
530 image, volume scattering dominates canola (bright green) while wheat fields show considerable  
531 double bounce (red).

532 Cloude and Pottier [168] approached characterization of target scattering by decomposing SAR  
533 response into a set of eigenvectors (which characterize the scattering mechanism) and eigenvalues  
534 (which estimate the intensity of each mechanism) [169]. Two parameters, the entropy (H) and  
535 the anisotropy (A), can be calculated from the eigenvalues. The entropy measures the degree of  
536 randomness of the scattering (from 0 to 1); values near zero are typical of single scattering  
537 (consider smooth bare soils) while entropy increases in the presence of multiple scattering  
538 events (consider a developing crop canopy). Anisotropy estimates the relative importance of the  
539 secondary scattering mechanisms. Most natural targets will produce a mixture of mechanisms  
540 although typically, one source of scattering dominates. Zero anisotropy indicates two secondary  
541 mechanisms of approximately equal proportions; as values approach 1 the second mechanism  
542 dominates the third [170]. The Cloude-Pottier decomposition also produces the alpha ( $\alpha$ ) angle  
543 to indicate the dominant scattering source [169]. Single bounce scatters (smooth soils) have alpha  
544 angles close to  $0^\circ$ ; as crop canopies develop the angle approaches to  $45^\circ$  (volume scattering)  
545 although some secondary or tertiary double-bounce (nearing  $90^\circ$ ) can be observed when canopies  
546 include well developed stalks. The Cloud-Pottier decomposition has been employed to retrieve  
547 the phenological stage of rice [171] and to identify harvested fields [172].

548

#### IV. APPLICATIONS

549 The models described in the previous section provide insight into scattering mechanisms, and  
550 in particular into the separation of the contributions from soil and vegetation. The ambiguity  
551 between these contributions is one of the main challenges to be addressed in applications of  
552 radar observations to agricultural landscapes. The WCM is popular in crop monitoring. Energy  
553 and Wave approaches have proved very valuable for forward modelling the backscatter from  
554 vegetation for soil moisture retrievals, and SAR decomposition methods are most popular in  
555 crop classification and monitoring approaches.

##### 556 *A. Regional vegetation monitoring using spaceborne scatterometry*

557 Several studies have used the ERS wind scatterometer to determine the fractional cover and  
558 seasonal cycles of vegetation. Woodhouse and Hoekman [173] used a mixed target modeling

559 approach to retrieve percentage vegetation cover over the Sahel region and the Hapex Sahel test  
560 area from ERS-1 WS data. A subsequent study in the Iberian Peninsula [174] yielded promising  
561 results for soil moisture retrieval but revealed that the performance in terms of vegetation cover  
562 parameters was site-specific. Frison et al. [175] showed that ERS WS data was more effective  
563 for monitoring the seasonal variation of herbaceous vegetation in the Sahel compared to SSM/I.  
564 The temporal signature of SSM/I observations were found to depend primarily on air and  
565 surface temperature, and integrated water vapor content. Biomass retrievals from SSM/I data  
566 were also poor due to the sensitivity of the employed semi-empirical model to soil moisture  
567 variations. Jarlan et al. [176] discussed the difficulty of estimating surface soil moisture and  
568 above-ground herbaceous biomass simultaneously without independent in-situ or remote sensing  
569 data to constrain one of the variables. In a subsequent study, soil moisture was estimated using  
570 MeteoSat data and a water balance model [177]. This allowed them to map vegetation water  
571 content and the herbaceous mass in the Sahelian through the nonlinear inversion of a radiative  
572 backscattering model yielding results that were consistent with NDVI observations. Grippa and  
573 Woodhouse [178] demonstrated that the inclusion of SAR data and ground measurements to  
574 estimate fractional cover in each of four cover classes allowed monthly vegetation properties to  
575 be retrieved from ERS WS backscatter at four test sites.

576 Higher frequency scatterometer data has also been used to monitor vegetation. Frohling et al.  
577 [40] showed that Ku-band backscatter from the SeaWinds-on-QuikSCAT scatterometer (QSCAT)  
578 could be used to monitor canopy phenology and growing season vegetation dynamics at 27 sites  
579 across North America. They found good agreement with MODIS LAI, but noted that the onset of  
580 growth was often detected earlier in the SeaWinds data than in the MODIS data. Similar results  
581 were observed by Lu et al. [179] in a similar study conducted at sites across China. Ringelmann  
582 et al. [180] identified increases in filtered QSCAT backscatter, associated with improved growing  
583 conditions, to estimate the planting dates in a semi-arid area in Mali. Hardin and Jackson [181]  
584 found seasonal change in backscatter from a savanna area in South America could be attributed  
585 due to variations in the dielectric constant of the grass itself accompanied by a strong contribution  
586 from soil moisture. Backscatter was found to decrease in the latter part of the season due to  
587 decreasing soil moisture and increased canopy attenuation.

588 It is important to note that the coarse resolution (typically around 25km) of the data used in  
589 these studies means that they are more suited to regional monitoring than field-scale monitoring.  
590 Nonetheless, they demonstrate that scatterometer data is suited for inter-annual monitoring of

591 the timing and evolution of the growing season which is useful for regional water resources  
592 management, food security monitoring, crop yield forecasting etc..

### 593 *B. Crop Classification*

594 The fine resolution of SAR observations make them better suited to field-scale crop classifi-  
595 cation. The primary advantage cited for integrating SARs with optical data in crop classification  
596 strategies is because microwave sensors are unaffected by cloud cover, making SARs a reliable  
597 source of data for scientific and operational needs. While this statement is correct, research has  
598 proven that optical data are not needed as input to a crop classifier as long as SAR configurations  
599 are optimized. As with optical approaches, if a SAR-only solution is to be successful multiple  
600 acquisitions through the growing season are needed [37]. At any single point in time two crops  
601 (e.g. wheat and oats) can have very similar backscatter. However, as the structure of the crop  
602 changes (especially during seed and fruit development), the backscatter changes. Classification  
603 can be performed based on these changes, using the variation in backscatter over time to  
604 distinguish one crop type from another. The number of images required depends upon the crops  
605 present and the complexity of the cropping system (for example number of crops, consistency of  
606 planting practices, presence of inter-cropping and number of cropping seasons per year). Le Toan  
607 et al. [182] showed that the distinctive backscatter changed between two ERS-1 SAR images  
608 during a rice growth cycle were enough to identify rice fields. By relating the backscatter to  
609 canopy height and biomass, they were also able to map rice fields at different growth stage. A  
610 subsequent study by Ribbes [183] found a lower dynamic range in RADARSAT images over rice  
611 compared to ERS-1, possibly due to polarization but found that RADARSAT was also potentially  
612 useful for rice-mapping. More recently, Bouvet et al. [184] used a series of ten X-band images  
613 from Cosmo SkyMed to map rice fields in the Mekong Delta, Vietnam. McNairn et al. [185]  
614 used multiple acquisitions of X-band and/or C-band data to deliver classification results with an  
615 overall accuracy of well over 90%, but in a simple corn-soybean-forage cropping system. In fact  
616 for this simple system, X-band imagery accurately (90-95%) identified corn only 6 weeks after  
617 seeding. However cropping systems can be much more complex, and in these circumstances it is  
618 important to include later images which capture periods of reproduction and seed development  
619 in the classifier, when crop structure changes are most apparent [186], [187].

620 As stated, successful classification requires multi-temporal SAR acquisitions to capture changes  
621 in crop phenology. When considering the SAR configuration, choice of frequency is very impor-

622 tant. This choice is not straightforward and the canopy (in terms of crop type and development)  
623 must be considered. Enough penetration is needed for microwaves to scatter into the canopy but  
624 when frequencies are too low, too much interaction occurs with the soil.

625 Inoue et al. [62] showed that, for rice, X- and K-band backscatter were sensitive to thin rice  
626 seedlings but poorly correlated with biomass and LAI which were better correlated with L- and C-  
627 band respectively. Data from several spaceborne SARs including ERS 1/2 SAR, Envisat ASAR,  
628 Radarsat and ALOS PALSAR have been used to map rice growth [182], [183], [188]–[190]. Jia  
629 et al. [191] favoured longer wavelengths at C-Band over X-Band for separating winter wheat  
630 from cotton. McNairn et al. [186] found that longer L-Band data was needed to accurately  
631 identify higher biomass crops (corn, soybean), although C-Band data was most suitable for  
632 separating lower biomass crops (wheat, hay-pasture). Because cropping systems include wide  
633 ranges of crops with varying volumes of biomass, researchers have consistently advocated for  
634 an integration of data at multiple frequencies to ensure high accuracy crop maps. Increases in  
635 accuracies have been reported when X- and C-Band data were integrated [191], C- and L-Band  
636 [186], [192], [193], X-, C- and L-Band [35] as well as C- and L- and P-Band [194]–[198]. The  
637 largest gains in accuracy are often observed for individual crop classes. In McNairn et al. [185],  
638 accuracies for individual crops increased up to 5% (end of season maps) and 37% (early season  
639 maps) when both X- and C-band were used together.

640 By and large, radar parameters which are responding to multiple or volume scattering within  
641 the crop canopy are the best choice for crop identification. Many studies have confirmed that the  
642 cross polarization (HV or VH) is the single most important polarization to identify the majority  
643 of crops [63], [102], [186], [199]–[201]. The greatest incremental increase in accuracy is then  
644 observed when a second polarization is added to the classifier [102], [199], [200]. Agriculture  
645 and Agri-Food Canada for example, integrates C-Band dual-polarization SAR (VV and VH from  
646 RADARSAT-2) with available optical data for their annual crop inventory [202]. This inventory  
647 is national in scale and is run operationally, delivering annual crop maps with overall accuracies  
648 consistently at or about 85%. Although the greatest improvements are observed when adding a  
649 second polarization when available, a third (such as HH) can increase accuracies for some crops  
650 [102], [186], [203]

651 Limited research has been published on the use of scattering decompositions within the context  
652 of crop classification. What has been presented has indicated small yet important incremental  
653 increases in accuracies. At L-Band, McNairn et al. [186] demonstrated that overall accuracies

654 improved up to 7% when decomposition parameters (Cloude-Pottier, Freeman-Durden) were  
655 used instead of the four linear intensity channels (HH, VV, VH, HV). Differences in the relative  
656 contributions of scattering mechanisms among the crops were observed leading to improved clas-  
657 sification. Liu et al. [163] used RADARSAT-2 data and the three Pauli components in a maximum  
658 likelihood classifier, applying this to a relatively simple cropping mix (corn, wheat, soybeans,  
659 hay-pasture). Two test years established an overall accuracy of 84-85%, using only these C-band  
660 data. Compact polarimetric (CP) data (in circular transmit-linear receive configuration) has been  
661 simulated from RADARSAT-2 C-band data and also assessed for crop classification. Using the  
662 Stokes vector parameters from synthesized CP data (4 images through the season) classification  
663 accuracies of 91% were reported with individual crop classification accuracies ranging from  
664 81-96% (corn, soybeans, wheat and hay-pasture) [204].

### 665 *C. Crop Monitoring*

666 Global, national and regional monitoring of crop production is critical for a host of clients.  
667 These clients include those concerned with food security where foresight into production esti-  
668 mates are needed to address potential food shortages, commodity brokers looking for information  
669 to facilitate financial decision making and agri-businesses which can more effectively deploy  
670 harvesting and transportation resources if production estimates are known in advance. Forecasting  
671 production is not a trivial task and as described in Chipanshi et al. [205] methods can be  
672 categorized as statistical, mechanistic or functional, with Earth observation data increasingly  
673 being used as data input into crop condition, production and yield forecasting. Agronomists are  
674 often interested in exploiting Leaf area Index (LAI) or biomass as surrogates, since both are good  
675 indicators of potential crop yield [206]. The structure of a crop canopy significantly impacts the  
676 intensity of scattering, type of scattering and phase characteristics. This structure is crop specific  
677 and varies as crop phenology changes. As such, research as far back as 1984 [207] and 1986 [208]  
678 has demonstrated a strong correlation between backscatter intensity and LAI. These researchers  
679 focused on higher frequency K- and Ku-band and noted strong correlations with the LAI of corn;  
680 weaker correlations being reported for wheat. This early research encouraged additional study  
681 into the sensitivity of SAR to LAI, leading to findings of strong correlations between C-band  
682 backscatter and LAI for wheat [209], corn and soybeans [210] and cotton [211]. Prasad [212]  
683 reported strong correlations between X-band backscatter and soybeans; Kim et al. [213] using  
684 L-, C- and X-band backscatter for soybeans. Liu et al. [163] examined RADARSAT-2 data to

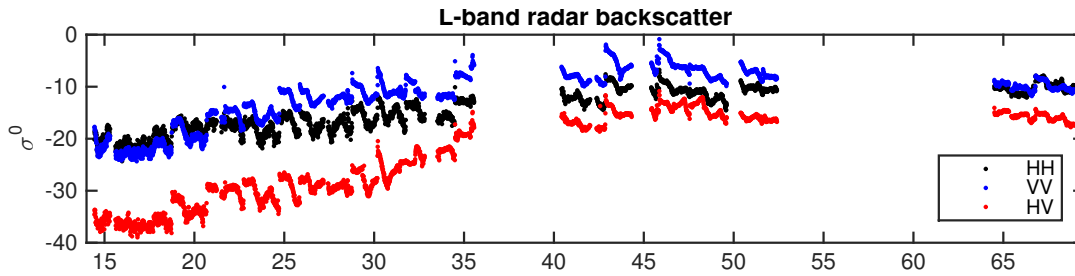


Fig. 4. Data collected in a corn canopy during Microwex10. Top: Surface (2.5cm) soil moisture, and LAI. Middle: Co- and cross-polarized backscatter  $\sigma^0$ . Bottom: RVI and vegetation water content.

685 track LAI development of corn and soybeans using Pauli decomposition parameters. Wiseman  
 686 et al. [214] observed strong correlations between C-band responses and the dry biomass of  
 687 corn, soybeans, wheat and canola. Much of the earliest research focused on linear like-polarized  
 688 responses (for example Ulaby et al. [207] and Paris [208] examined HH and VV polarizations).  
 689 Scattering from crop canopies is a result of multiple scattering from within the crop canopy,  
 690 and between the canopy and soil. As such, repeatedly the highest correlations with LAI and  
 691 biomass have been found for SAR parameters indicative of these multiple scattering events. These  
 692 parameters include HV or VH backscatter, pedestal height, volume scattering components from  
 693 decompositions and entropy ( [195], [196], [209], [210], [214]–[216] all using C-band). Although  
 694 SAR parameters responsive to volume scattering have proven most sensitive to crop condition  
 695 indicators such as LAI and biomass, a few researchers have reported success in combining  
 696 polarizations in the form of ratios. This has included a C-band HH/VV ratio for wheat biomass  
 697 [21], wheat LAI [217] and rice LAI [218]. C-HV/HH proved sensitive to the LAI of sugarcane  
 698 [219].

699 In 2009, Kim and van Zyl [220] introduced the Radar Vegetation Index (RVI) whereby RVI  
 700 is expected to increase (from 0 to 1) as volume scattering increases due to canopy development.  
 701 RVI is defined as:

$$RVI = \frac{8\sigma_{hv}^0}{\sigma_{hh}^0 + 2\sigma_{hv}^0 + \sigma_{vv}^0} \quad (6)$$

702 where  $\sigma_0$  is SAR intensity for each transmit (h or v) and receive (h or v) polarization.

703 Figure 4 shows a time series of RVI calculated from data collected during Microwex 10 with  
 704 the UF-LARS. Though HV is typically lower than co-polarized backscatter, it is clearly most  
 705 sensitive to the increasing biomass, indicated by increasing LAI. RVI is less than 0.2 up to 30

706 days from planting because the magnitude of HV is much lower than the co-polarized backscatter.  
707 After this date, RVI increases steadily until the plant reaches full growth. Fluctuations in RVI  
708 reflect changes in soil moisture (influencing co-pol backscatter), and vegetation water content  
709 (influencing cross-pol backscatter). RVI has been statistically correlated with the plant area and  
710 biomass of some crops [214], [221], [222]. It has also been used to estimate VWC for soil  
711 moisture studies e.g. [223], [224].

712 Radar response from crop canopies can saturate at higher LAI or biomass. This means that as  
713 the crop continues to accumulate plant matter, the radar backscatter is no longer responsive to  
714 these increases. The exact point of saturation is crop and frequency specific. For corn, McNairn et  
715 al. [102] found that C-HH saturated at a height of one meter. When considering LAI, saturation  
716 has been reported at LAI of 2-3 (Ulaby et al., [207], using K-band), LAI of 3 for corn and  
717 soybeans [210] and LAI of 3 for rice [135]. Not all research has reported saturation; for winter  
718 wheat backscatter continued to be sensitive to crop development throughout the season [96].  
719 Although saturation is problematic when monitoring some crops during the entire season, a  
720 critical window for crop yield forecasting is during the period of rapid crop development up  
721 until peak biomass accumulation. Wiseman et al. [214] reported exponential increases in C-band  
722 responses in the early season when biomass accumulation accelerated, especially for parameters  
723 such as entropy (corn and canola) and HV backscatter (soybeans). Thus SAR-based estimates  
724 of LAI, even if restricted to periods prior to peak biomass accumulation, will be useful in  
725 monitoring crop productivity. These studies which reported a sensitivity of SAR to LAI and  
726 biomass gave rise to efforts to model and eventually estimate biophysical parameters indicative  
727 of crop condition. The Water Cloud Model (WCM) has been a choice approach to estimate crop  
728 parameters given its relative simplicity to model and invert. The influence of soil moisture on SAR  
729 response dissipates as the canopy develops. Prevot et al. [96] reported that at X-band once the  
730 LAI of wheat reached four, soil contributions were negligible. At C-band, once the LAI of corn  
731 and soybeans reached three, 90% of scattering originates from the canopy [210]. Nevertheless,  
732 considering the requirement to model the entire growth cycle, it remains important to consider  
733 soil moisture contributions within the WCM. Ulaby et al. [207] demonstrated that when LAI  
734 is less than 0.5, backscatter is dominated by soil moisture contributions. One approach to LAI  
735 retrieval with the WCM is to provide ancillary sources of soil moisture. This is particularly  
736 effective when the number of available SAR parameters is not sufficient to retrieve multiple  
737 unknown variables modeled by the WCM. This approach was demonstrated by Beriaux et al.

738 [137]. Here VV backscatter was used to estimate the LAI of corn, using ancillary sources of soil  
739 moisture. LAI errors (RMSE in  $m^2/m^2$ ) were reported as 0.69 (using soil moisture from ground  
740 penetrating radar), 0.88 (using field measurements) and 0.9-0.97 (using moisture modeled by  
741 SWAP). If multiple SAR parameters are available, LAI can be retrieved without provision of  
742 ancillary soil moisture data. Prevot et al. [96] did so using two frequencies (X-band and C-band)  
743 and reported a RSME for retrieval of LAI for winter wheat as 0.64  $m^2/m^2$ . Soil moisture was  
744 also retrieved (RSME of 0.065  $cm^3/cm^3$ ). In a slightly modified approach, Hosseini et al. [136]  
745 used multiple polarizations from RADARSAT-2 and an airborne L-band sensor to invert the  
746 WCM without the need for ancillary moisture data. In this case, LAI was accurately estimated  
747 using C-VV and C-VH backscatter for corn (RMSE of 0.75  $m^2/m^2$ ) and soybeans (RMSE of  
748 0.63  $m^2/m^2$ ). Errors using L-band were at or above RMSE of 1, perhaps indicating too much  
749 penetration for accurate LAI retrieval for these canopies. Research continues in this domain, yet  
750 it is evident that SAR can provide estimates on LAI to support the monitoring of crop condition.  
751 In fact, error statistics for retrieval of LAI for corn and soybeans using RADARSAT-2 [136]  
752 were slightly lower than those achieved using optical RapidEye data [225], both experiments  
753 occurring in Canadian cropping systems.

754 Beyond LAI, Polarimetric SAR (PolSAR) has proved very valuable for monitoring phenolog-  
755 ical stages of rice [226]–[231] and other crops [221], [232]–[234]. Recently, Vicente-Guijalba  
756 et al [235] presented a dynamic approach for agricultural crop monitoring. First, a dynamical  
757 model for crop phenological change is extracted from a reference dataset (e.g. a stack of SAR  
758 images). Then, this model is constrained by input data using an extended Kalman filter (EKF)  
759 to estimate the crop phenological stage on a continuous scale in real time. They demonstrated  
760 using Radarsat data from AgriSAR2009 that the approach worked well for wheat and barley.  
761 For oats, the sensitivity was only sufficient in the first and last stages. In related studies, data  
762 fusion [236] and data assimilation [237], [238] techniques were also successfully used to extract  
763 key dates or phenological stages from stacks of SAR images. Mascolo et al. [239] presented  
764 a novel methodology that uses distances among covariance matrices derived from series of  
765 PolSAR images to identify both the phenological intervals to be estimated. It also determines  
766 the training sets for each interval and the intervals are then classified by the complex Wishart  
767 classifier. The advantage is that this method obviates the need to identify specific PolSAR  
768 features. They demonstrated, using RADARSAT-2 data from the AgriSAR2009 campaign, that  
769 this methodology can be used to retrieve the phenological stages of four different crop types

770 namely oat, barley, wheat, and corn. Finally, Polarimetric SAR interferometry, in which the  
 771 strengths of interferometry are combined with those of polarimetric SAR, has been put forward  
 772 to address some of the shortcomings of polarimetric SAR in agricultural monitoring [240].  
 773 PolInSAR yields information about the localization of the scattering centers, and hence the  
 774 vertical structure of the plant. Lopez-Sanchez and Ballester-Berman [240] argue that this may  
 775 be used to overcome the saturation effects observed in PolSAR and to monitor plant phenological  
 776 stage.

#### 777 *D. Soil Moisture*

778 Soil moisture is important in its own right for agricultural scheduling and water resources  
 779 management [241] and drought monitoring [242]. Furthermore, soil moisture observations can  
 780 be used to account for the influence of drought conditions on crop yield forecasts [243]–[245].  
 781 The soil moisture dataset derived from the ERS 1/2 wind scatterometers and the Advanced  
 782 Scatterometer (ASCAT), provides one of the longest-duration global records of soil moisture  
 783 and is the only operational global soil moisture product derived from radar observations [246].  
 784 It is based on an empirical soil moisture retrieval algorithm that accounts for seasonality in  
 785 the influence of vegetation on the sensitivity of backscatter to soil moisture [247]. First, the  
 786 entire record of backscatter coefficients from the ERS Wind Scatterometer is extrapolated to a  
 787 reference angle of  $40^\circ$ , yielding a time series  $\sigma^0(40, t)$ . The highest and lowest values of  $\sigma^0(40, t)$   
 788 for each grid cell,  $\sigma_{wet}^0(40, t)$  and  $\sigma_{dry}^0(40, t)$ , are identified. The first is generally independent of  
 789 vegetation status, while  $\sigma_{dry}^0(40, t)$  varies seasonally with vegetation phenology. Assuming that  
 790  $\sigma^0(40)$  and the surface soil moisture are linearly related, the relative moisture content of the  
 791 surface (0.5-2cm thick) layer is given by:

$$m_s(t) = \frac{\sigma^0(40, t) - \sigma_{dry}^0(40, t)}{\sigma_{wet}^0(40, t) - \sigma_{dry}^0(40, t)} \quad (7)$$

792 This approach was developed for a study in the Iberian peninsula [247]. In a subsequent study,  
 793 the approach was validated using an extensive in-situ dataset from Ukraine [248] and a soil water  
 794 index (SWI) was introduced to provide a measure of profile soil moisture. SWI is obtained as  
 795 a convolution of the time series of surface moisture content with an exponential filter function  
 796 such that

$$SWI(t) = \frac{\sum_i m_s(t_i) e^{-(t-t_i)/T}}{\sum_i e^{-(t-t_i)/T}} \quad (8)$$

797 for  $t_i \leq t$ , where  $m_s$  is the surface soil moisture from the ERS WS at time  $t_i$ ,  $T$  is some  
798 characteristic time length between 15 and 30 days. Wagner et al. [249] evaluated both products  
799 over West Africa. They demonstrated that the temporal and spatial distributions of the estimated  
800  $m_s$  and  $SWI$  captured the influence of the wet and dry seasons and that the estimated slope  
801 parameters were consistent with the distribution of land cover. Wagner et al. [250] presented first  
802 global, multiannual soil moisture data set (1992–2000) from satellite remote sensing. Due to the  
803 lack of a global network of in-situ validation data, the estimated soil moisture was compared  
804 with observed monthly precipitation data, and monthly soil moisture obtained from a dynamic  
805 global vegetation model. A comparison of anomalies in  $SWI$  and precipitation anomalies yielded  
806 correlations up to 0.9 in tropical and temperate regions. Though spurious effects were observed  
807 in steppe and desert climates, this study illustrated the potential value of spaceborne scatterometer  
808 data for soil moisture estimation. Following the launch of the first of three METOP satellites  
809 in October 2006, Bartalis et al. [251] used the parameters derived from eight years of ERS  
810 scatterometer data, to produce first global soil moisture maps from the METOP-A Advanced  
811 Scatterometer (ASCAT) commissioning data. Comparison of the ASCAT-derived surface soil  
812 moisture to rainfall and NDVI data suggested that the approach developed for the ERS scat-  
813 terometer could be applied to ASCAT data with minimal adaptations required to the processing  
814 chain and configuration.

815 Naemi et al. [252] made several improvements to address shortcomings in the original algo-  
816 rithm to yield the so-called WARP5 model.

817 Soil moisture estimates derived from both the ERS WS and MetOp ASCAT, using a newer  
818 WARP5.2 are key components of the European Space Agency Climate Change Initiative (ESA  
819 CCI) soil moisture product [253]. A recent study by Vreugdenhil et al. [254] highlighted the  
820 need to develop to better account for the influence of vegetation dynamics on soil moisture  
821 retrieval, particularly in areas where there is significant interannual variability in vegetation.

822 NASA’s Soil Moisture Active Passive (SMAP) mission was launched on January 31, 2015  
823 with an L-band radiometer and L-band SAR on board. The SMAP baseline algorithm for the  
824 radar-only soil moisture product was to use a multi-channel datacube retrieval approach outlined  
825 by Kim et al. [255], [256]. Forward backscatter models for 16 vegetation classes and bare soil  
826 are used to simulate backscatter as a function of the real part of the soil dielectric constant ( $\epsilon_r$ ),  
827 roughness ( $s$ ), and vegetation water content ( $VWC$ ). Scattering from each of the vegetation  
828 types is simulated using the methods described in Section III.B, and based on data collected

829 from field campaigns. For retrieval  $\sigma_{HV}$  or ancillary data is used to determine  $VWC$  and a time  
830 series of co-polarized backscatter is used to determine a single value for  $s$  and a time series of  
831  $\epsilon_r$  by minimizing the difference between simulated and observed backscatter [6]. In addition to  
832 this baseline algorithm, the change detection approaches of van Zyl and Kim [257] and Wagner  
833 et al. [247] are considered as optional algorithms. Unfortunately, the failure of the radar in July  
834 2015 means that SMAP products are currently limited to those from the radiometer alone.

## 835 V. CHALLENGES AND OPPORTUNITIES

### 836 A. Resolution of spaceborne scatterometry data

837 The coarse resolution of spaceborne scatterometer observations remains a challenge. However,  
838 resolution enhancement [258], [259], data assimilation [260]–[262] and downscaling approaches  
839 [263] offer new possibilities in terms of extracting field-scale or, at least, finer-scale information  
840 from coarse scatterometer observations for agricultural applications.

### 841 B. Limitations of operational SAR applications

842 Spatial and temporal coverage remains a huge challenge for operational SAR applications  
843 in agriculture. The results discussed here illustrate that theoretically, radar data is an excellent  
844 option for crop type monitoring to support production estimates, and to monitor crop condition.  
845 The quality of multi-frequency radar data retrievals in these applications is sufficiently high to  
846 obviate the need for optical data. The recent launches of Cosmo Sky-Med (4 day revisit time) and  
847 Sentinel 1a and 1b (6 day revisit time) have greatly improved temporal coverage. Nonetheless,  
848 spatial and temporal availability of data remains a barrier to operational global, regional or even  
849 national monitoring. For example, the current state-of-the-art operational monitoring performed  
850 by Agriculture and AgriFood Canada still relies on the integration of radar and optical data.

851 Furthermore, to transition from scientific applications to operational monitoring, the current  
852 model (i.e. WCM) needs to be adapted so that it can be applied for a wider range of cropping  
853 systems. Finally, the extensive history of using optical data in agriculture means that users  
854 are familiar with the processing and interpretation of optical imagery. The complexity of SAR  
855 scattering means that applications specialists in agricultural monitoring generally consider in-  
856 terpretation of radar images more difficult than optical images. This is a major barrier to the  
857 widespread adoption of radar for operational monitoring, most of which is carried out by national

858 institutions. User community participation and capacity-building activities are needed to ensure  
859 that radar products are provided to users in a format that they can readily use.

### 860 *C. Water stress monitoring using spaceborne radar*

861 An emerging topic of research is the potential use of diurnal variations in backscatter to identify  
862 the onset of water stress. Friesen [264] identified statistically significant diurnal differences in  
863 backscatter from the ERS 1/2 wind scatterometer over West Africa. A hydrological model, and  
864 a degree-day model were used to demonstrate that the largest differences coincided spatially and  
865 temporally with the onset of water stress [264]. A sensitivity study using the MIMICS model  
866 showed that the variations may be attributed to variations in the water content (and hence relative  
867 permittivity) of the leaves and trunks [265]. The challenge remains to disentangle the artefacts of  
868 WS pre-processing from the influence of variations in dielectric properties and geometric changes  
869 in the canopy due to the forest's physiological response to water stress. Diurnal variations have  
870 been detected in higher-frequency spaceborne observations too [3], [266]–[268]. Frohling et al.  
871 [2] identified a decrease in backscatter over the southwestern Amazon forest during the 2005  
872 drought. The most significant anomalies, with respect to interannual variability, were in the  
873 morning backscatter anomalies. Strong spatial correlation with water deficit anomalies suggested  
874 that these anomalies were due to drought - hypothesizing, similarly to Friesen [264], that the  
875 changes were due to changes in water relations within the tree in response to stress.

876 In the agricultural context, diurnal differences in backscatter were also observed in agricultural  
877 canopies in tower-based measurements as early as the 1970s [64], [269], and were attributed  
878 to loss of canopy moisture during the day due to transpiration. A more recent study in an  
879 agricultural maize canopy found diurnal changes in bulk VWC up to 30 % and leaf VWC up to  
880 40% during a period of water stress [28]. Water cloud model simulations were used to illustrate  
881 that the variations in leaf VWC had a significant impact on total backscatter, particularly at  
882 C-band and higher frequencies. Schroeder et al. [270] normalized ASCAT backscatter to  $54^\circ$   
883 to maximize sensitivity to the slope factor. Recall from Wagner [247] that the slope factor  
884 reflects variations in vegetation water content or phenology. Schroeder et al. found that negative  
885 anomalies in  $\sigma^0(54)$ , particularly during the morning overpasses, were spatially and temporally  
886 consistent with the drought patterns observed in 2011 and 2012 by the U.S. Drought Monitor.  
887 Additional research is needed to relate the observed backscatter variations with the underlying

888 plant response to drought, and hence to explore the potential of scatterometer and SAR data at  
889 different frequencies to identify water stress at regional and field scales respectively.

#### 890 *D. New opportunities with ASCAT*

891 Twenty five years since the launch of the Active Microwave Instrument (AMI) on ERS-  
892 1, sensors that were primarily launched for ocean applications are at the core of operational  
893 remote sensing for land surface monitoring. The continuation of ASCAT on MetOp will provide  
894 essential operational soil moisture data for the meteorological, hydrological and land monitoring  
895 communities [271]. Recent research by Vreugdenhil [254] demonstrates that there is valuable  
896 information about vegetation dynamics in the ASCAT observations. The ability to quantitatively  
897 exploit this information could lead to improved soil moisture retrieval and vegetation phenology  
898 monitoring.

#### 899 *E. Vegetation dynamics from RapidScat on ISS*

900 Paget and Long [3] recently mapped diurnal variations in Ku-band backscatter observations  
901 from RapidScat. Significant variations were observed across several vegetation biomes. Though  
902 previous studies have indicated that diurnal variations at several frequencies could be due to  
903 variations in water dynamics [264], [272], [273], uncertainty still surrounds the relationship  
904 between plant water relations, variations in dielectric properties, and the observed backscatter [2],  
905 [3], [265], [274]. Understanding what drives these diurnal backscatter variations is the first step  
906 to exploiting RapidScat for agricultural applications. Furthermore, their exploitation would also  
907 yield valuable insight into the potential value of the ISS as a platform for vegetation monitoring  
908 using radar.

#### 909 *F. New C-band SAR missions*

910 Two new C-band SAR constellations offer global high-resolution imagery at an unprecedented  
911 spatial and temporal resolution thereby offering the potential to more accurately pinpoint growth  
912 stages and monitor biomass accumulation, vegetation water content etc.. The two satellites of  
913 ESA's C-band Sentinel-1 Mission were launched in 2014 and 2015 respectively. They are the first  
914 in a series of operational satellites in the frame of ESA's Global Monitoring for Environment  
915 and Security Space Component programme. The two satellites are in the same orbital plane  
916 providing an average revisit time of two days above 45° N/S and global exact repeat coverage

917 every two weeks. It has four imagine modes: the Interferometric Wide-swath model (IW), Wave  
918 Mode (WM), Strip Map mode (SM) or Extra-Wide (EW) swath model. Apart from the single-  
919 polarization WM, all modes have dual polarization with VV and VH as the default [275].  
920 Canada's three-satellite RADARSAT Constellation Mission (RCM) is scheduled for launch in  
921 2018. It will support the operational requirements of the Government of Canada and to provide  
922 data continuity for existing users of RADARSAT-1 and RADARSAT-2 [276]. RCM will have a  
923 range of modes from wide area surveillance modes (500 km swath) to spotlight modes (5 km  
924 swath). Single or dual polarization acquisitions (HH + HV or VV + VH or HH + VV) are possible  
925 for each mode. The constellation also provides access to both quad-polarization and compact  
926 polarization (CP) modes. RCM will have a 12-day repeat cycle and with three satellites, 4-day  
927 coherent change detection will be possible. From Section IV, it is clear that the exploitation  
928 of SAR data, particularly Radarsat1 and Radarsat 2 data, has significantly contributed to our  
929 understanding of scattering mechanisms in vegetation. Similarly, knowledge generated from the  
930 use of Sentinel-1 and RCM can be transferred to improve our understanding of scatterometry and  
931 facilitate increase exploitation of the data collected by ASCAT on MetOp and other spaceborne  
932 scatterometry missions.

### 933 *G. Combined SMAP/Sentinel-1 soil moisture*

934 One of the objectives of NASA's SMAP mission was to combine the radiometer and radar  
935 observations to produce a merged soil moisture product at 9km resolution. Sentinel-1 observations  
936 have been proposed as a potential substitute for SMAP radar observations in this combined  
937 product since the radar failure in July 2015 [277]. However, there are several differences between  
938 the SMAP radar data and the Sentinel-1 SAR data that will need to be addressed. In addition to  
939 the difference in frequency between the two radars, and the incidence angle diversity of Sentinel-  
940 1, the main challenge is that the two instruments are not in the same orbit. Any downscaling  
941 approach must therefore be robust enough to merge acquisitions from the SMAP radiometer and  
942 Sentinel-1 radar that are separated by hours of even days. Combined multi-angle, C- and L-band  
943 radar observations from tower-based scatterometers could play an important role in developing  
944 and validating proposed downscaling approaches to take these differences into account.

## 945 *H. Scattering models for vegetation*

946 The persistent dilemma in terms of radar applications for vegetation is choosing an appropriate  
947 model. The Water Cloud Model remains widely used despite, if not because, of its simplicity.  
948 However, its key assumptions regarding the distribution of moisture in the canopy are generally  
949 not valid. The more theoretical energy and wave-based approaches remain primarily in the  
950 research domain due to the large number of input parameters required (e.g. dielectric properties  
951 of soil and vegetation, geometry etc.. This data collection requirement may be possible during  
952 intensive field campaigns, but it is too time consuming and expensive to be performed regularly  
953 and for all possible vegetation cover types. Furthermore, the representations of the canopy in  
954 energy and wave-based models are still simplifications of reality. For emerging applications, it  
955 is significant that the relationship between these parameters and vegetation (particularly water)  
956 dynamics is currently not well understood. A new approach to modeling is needed that reflects the  
957 known non-uniformity and dynamic profile in moisture content, and the importance of multiple-  
958 bounce between the soil surface and overlying vegetation. However, to ensure that the model is  
959 universally applicable, it needs to be as simple to parameterize and use as the WCM.

## 960 *I. Radar tomography*

961 From the discussions in the previous sections becomes clear that the main limitation of  
962 conventional single- or quad-polarimetric acquisitions, arises from the fact that they do not  
963 provide the required dimensionality to resolve unambiguously the multiple and/or complex  
964 scattering processes ongoing at different polarisations and frequencies. A potential solution  
965 to this are multi-angular acquisitions that allow the reconstruction of the 3D reflectivity of  
966 volume scatterers by means of tomographic techniques. In the context of agricultural crops the  
967 first experiments and demonstrations were performed by means of ground based scatterometers  
968 in indoor and outdoor set-ups [278]. More recently, the developments in SAR technology and  
969 data processing allowed first tomographic airborne SAR experiments over agricultural fields even  
970 at higher frequencies [279], [280].

971 Airborne tomographic SAR experiments are mostly carried out by displacing the multiple  
972 acquisitions on a linear configuration such that the variation of the radar look angle amounts  
973 to a small fraction of a degree between consecutive acquisitions [281]. In conventional linear  
974 tomography the 3D reflectivity is inverted from the multi-acquisition data vector by means of a  
975 Fourier-based approach [281], [282]. In this case, the spatial resolution in the elevation direction

976 (also referred to as cross-range direction i.e. the direction perpendicular to the radar LoS) is  
 977 defined by the length of the formed synthetic aperture  $L_X$ , that corresponds to the maximum  
 978 separation (in elevation) between the acquisitions:

$$\delta = \frac{\lambda}{2L_X} r_0 \quad (9)$$

979 where  $\lambda$  is the radar wavelength and  $r_0$  the distance between radar and scatterer. For example, in  
 980 order to achieve, with an X-band radar, a resolution in elevation of 1m at a distance  $r_0 = 5km$  an  
 981 aperture of 150m is required. While the maximum separation between the acquisitions is defined  
 982 by the resolution requirement, the number of acquisitions needed for tomographic imaging is  
 983 given by the distance between the acquisitions required to fulfil Nyquist sampling. For a scatterer  
 984 (e.g. agricultural field) with height  $H_X$  in elevation, the minimum required distance between the  
 985 acquisitions is given by [281]:

$$d_X = \frac{\lambda}{2H_X} r_0 \quad (10)$$

986 Equations 9 and 10 make it clear that the lower heights of agricultural vegetation require high  
 987 vertical resolutions and demand a larger number of acquisitions. In the example used above for  
 988 mapping a  $H_X = 3m$  tall agriculture field, a minimum distance of 25m between the acquisitions  
 989 is required so that in total 7 acquisitions are at least required assuming a uniform spacing among  
 990 them.

991 For each SAR image pixel, the reflectivity profile can be inverted from the related multi-  
 992 acquisition data vector by means of a Fourier-based approach [281], [282]. However, the re-  
 993 constructed profile will in general be affected by the presence of sidelobes that can lead to  
 994 misinterpretations of the reflectivity distribution. On the other hand, a resolution better than the  
 995 one provided by the tomographic aperture [see 9] is desired, especially for small vegetation vol-  
 996 umes like crops. In order to improve the reconstruction performance and to relax the acquisition  
 997 requirements, adaptive reconstruction algorithms have been proposed. One interesting and pop-  
 998 ular example is the Capon spectral estimator, a widely employed low-complexity solution [282].  
 999 More recently, Compressive Sensing reconstruction techniques that allow a high-performance  
 1000 reconstruction even with a very low number of acquisitions (that may even not fulfil the Nyquist  
 1001 sampling condition) have been proposed [283]. Both algorithms have been demonstrated to  
 1002 greatly improve the reconstruction of the reflectivity profile in terms of side-lobe cancellation  
 1003 and resolution enhancement, at the cost of some (generally acceptable) radiometric non-linearity.

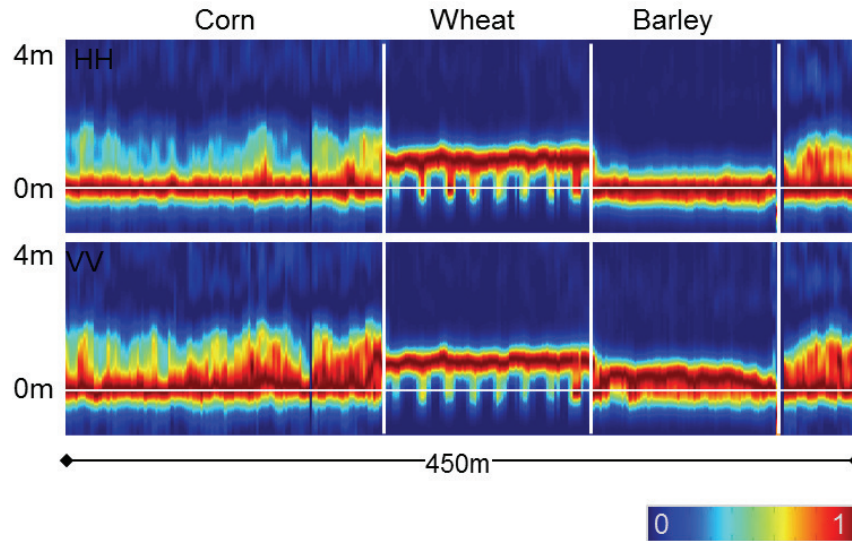


Fig. 5. Normalised tomographic reflectivity profile across three fields (corn, wheat and barley) at X-band with a vertical resolution of  $\delta_z = 0.5m$  at HH (top) and VV (bottom).

1004 Figure 5 shows a Capon tomographic reflectivity profile across three fields (corn with a  
 1005 physical height of 1.8 m at the time of the acquisition, wheat with a height of 0.8m, and barley  
 1006 with a height of 0.8m) at X-band with a vertical resolution of 0.5 m formed by 9 airborne SAR  
 1007 acquisitions performed on the 3rd of July 2014 over the Wallerfing test site (South Germany).  
 1008 Looking at the profile, one can clearly distinguish the different scattering processes. The corn  
 1009 field, which is still in its early development stage, is dominated by dihedral scattering (by HH  
 1010 dominated scattering located on the ground). Over the wheat field, surface scattering on the top  
 1011 layer is ongoing and the row spacing is clearly visible. Over the dry barley field, the vegetation  
 1012 at HH is almost "invisible" and only appears weakly in VV [280].

1013 Figure 5 illustrates that tomographic imaging has the potential to make a critical and unique  
 1014 contribution to our understanding of scattering from agricultural scenes as it allows us to identify  
 1015 the dominant scattering processes as well as their change in time at different polarisations and  
 1016 frequencies. This is essential for understanding propagation and scattering within agriculture  
 1017 vegetation and interpreting correctly conventional back-scattering signatures. The availability  
 1018 of multi-temporal tomographic acquisitions is especially critical when it comes to determine  
 1019 processes that effect the dielectric and/or geometric characteristics of the scatterers.

1020 However, the large number of acquisitions, combined with the fast temporal evolution of

1021 agricultural plants, limits the application of radar tomography to rather small-scale ground-based  
1022 and/or airborne experiments. Spaceborne repeat-pass implementations are limited by temporal  
1023 decorrelation that has more of an effect on the higher frequency range preferred for agricultural  
1024 vegetation applications. An interesting alternative - proposed and used for forest tomography -  
1025 are single pass spaceborne configurations that are able to provide tomographic imaging based  
1026 on (single pass) interferograms acquired at consecutive repeat-pass cycles [282]. However the  
1027 fast development of agriculture plants requires very short repeat-pass cycles in order to avoid  
1028 changes in the 3D-reflectivity due to the plant evolution. Accordingly, until the next generation  
1029 of multi-static spaceborne SAR configurations becomes operational, the availability and coverage  
1030 of tomographic data will be limited but significant for the development of simplified inversion  
1031 approaches invertible with a "slimmer" in terms acquisitions observation space [240], [284]–  
1032 [287] .

### 1033 *J. Innovative ground measurements*

1034 Several innovative ground measurement techniques offer new insight into vegetation dynamics,  
1035 specifically biomass accumulation and vegetation water content variations, i.e. GPS-IR [288]–  
1036 [290], wireless networks [291], and COSMOS [292], [293]. These ground-based sensors yield  
1037 indirect, though continuous estimates of VWC and biomass which could fill the gaps between  
1038 less frequent destructive sampling. Data from these new sensors with conventional measurements  
1039 of plant architecture and moisture profile could be combined with continuous tower-based  
1040 scatterometry to study sub-daily variations in backscatter and to develop new models that account  
1041 for variations at scales not considered in the current formulation of the Water Cloud Model.

## 1042 VI. CONCLUSIONS

1043 Ground-based and aircraft-based experiments have been central to our understanding of backscat-  
1044 ter from vegetation and how it depends on system parameters (frequency, polarization, incidence  
1045 and azimuth angle) and surface characteristics (soil moisture and roughness, vegetation moisture  
1046 and geometry). They have also played a crucial role in the development and validation of  
1047 models and decomposition methods. This has enabled the development of radar as a tool  
1048 for agricultural applications, particularly crop classification, crop growth monitoring and soil  
1049 moisture monitoring.

1050 Though spaceborne scatterometry has been used to monitor vegetation phenology at regional  
1051 scales, field scale classification and crop monitoring has primarily exploited spaceborne SAR due  
1052 to its fine resolution. Limited coverage, until now, has hindered widespread operational use. The  
1053 rather long revisit time of SAR missions to date has limited their use for soil moisture monitoring.  
1054 Despite their coarse resolution, soil moisture products from the ERS 1/2 wind scatterometer  
1055 and ASCAT on MetOp have become a data cornerstone in hydrological and climate studies.  
1056 Recent advances in both SAR and scatterometry demand improved representation of vegetation  
1057 dynamics.

1058 The recent launch of the Sentinel-1 satellites and the upcoming Radarsat Constellation mean  
1059 that C-band SAR observations will be available with unprecedented revisit time opening the  
1060 possibility of observing vegetation dynamics at a finer temporal scale than ever before. At  
1061 the same time, several studies using spaceborne scatterometry data (C-band and K-band) have  
1062 revealed that backscatter is sensitive to vegetation water content variations and in particular to  
1063 water stress. These developments demand the ability to understand and simulate scattering from  
1064 vegetation at finer temporal scales than ever before.

1065 To ensure that we can exploit both SAR and scatterometry data to its full potential, we need to  
1066 develop models that consider vegetation as a dynamic scattering medium rather than a medium  
1067 that changes slowly over the growing season. Being able to quantify the influence of water  
1068 dynamics on backscatter could lead to improved soil moisture retrievals, and reduce uncertainty  
1069 in crop classification and monitoring applications. It would also stimulate the development of  
1070 regional scale water stress monitoring based on spaceborne scatterometry. Innovative methods  
1071 like GPS-IR and radar tomography can play a vital role in characterizing the dynamics of  
1072 the moisture distribution. Coupling these with ground-based scatterometry experiments would  
1073 provide a detailed and rich dataset with which to revisit the modeling of backscatter of vegetation.  
1074 Improvements in current applications and the development of emerging applications will facilitate  
1075 the exploitation of the new generation of SAR satellites, and the continued exploitation of the  
1076 historic and operational data record from spaceborne scatterometry.

1077

#### ACKNOWLEDGMENT

1078 Susan Steele-Dunne's research is supported by a Vidi grant (ref.14126) from the Dutch Tech-  
1079 nology Foundation STW, which is part of the Netherlands Organisation for Scientific Research  
1080 (NWO), and which is partly funded by the Ministry of Economic Affairs. The work of A.

1081 Monsivais-Huertero was supported by the National Council of Science and Technology of Mexico  
1082 (CB-2010-155375).

1083

## REFERENCES

- 1084 [1] J. Friesen, S. C. Steele-Dunne, and N. van de Giesen, "Diurnal Differences in Global ERS Scatterometer Backscatter  
1085 Observations of the Land Surface," *IEEE Transactions on Geoscience and Remote Sensing*, vol. 50, no. 7, pp. 2595–2602,  
1086 Jul. 2012.
- 1087 [2] S. Frolking, T. Milliman, M. Palace, D. Wisser, R. Lammers, and M. Fahnestock, "Tropical forest backscatter anomaly  
1088 evident in SeaWinds scatterometer morning overpass data during 2005 drought in Amazonia," *Remote Sensing of  
1089 Environment*, vol. 115, no. 3, pp. 897–907, Mar. 2011.
- 1090 [3] A. C. Paget, D. G. Long, and N. M. Madsen, "RapidScat Diurnal Cycles Over Land," *IEEE Transactions on Geoscience  
1091 and Remote Sensing*, vol. 54, no. 6, pp. 3336–3344, Jun. 2016.
- 1092 [4] F. Ulaby, R. More, and A. Fung, *Microwave Remote Sensing: Active and Passive. Vol. I: Microwave Remote Sensing  
1093 Fundamentals and Radiometry*. Boston, MA: Artech House, 1986.
- 1094 [5] F. Ulaby, P. Dubois, and J. van Zyl, "Radar mapping of surface soil moisture," *J. Hydrology*, vol. 184, no. 1-2, pp. 57–84,  
1095 October 1996.
- 1096 [6] S.-b. Kim, J. van Zyl, S. Dunbar, E. Njoku, J. Johnson, M. Moghaddam, J. Shi, and  
1097 L. Tsang, "SMAP L2 & L3 Radar Soil Moisture (Active) Data Products," 2012. [Online]. Available:  
1098 [https://media.asf.alaska.edu/uploads/12%263\\_sm\\_a\\_initrel\\_v1\\_5.pdf](https://media.asf.alaska.edu/uploads/12%263_sm_a_initrel_v1_5.pdf)
- 1099 [7] F. Ulaby, "Radar response to vegetation," *IEEE Transactions on Antennas and Propagation*, vol. 23, no. 1, pp. 36–45,  
1100 Jan. 1975.
- 1101 [8] F. Ulaby, T. Bush, and P. Batlivala, "Radar response to vegetation II: 8-18 GHz band," *IEEE Transactions on Antennas  
1102 and Propagation*, vol. 23, no. 5, pp. 608–618, Sep. 1975.
- 1103 [9] A. Joseph, R. van der Velde, P. O'Neill, R. Lang, and T. Gish, "Effects of corn on C- and L-band radar backscatter: A  
1104 correction method for soil moisture retrieval," *Remote Sensing of Environment*, vol. 114, no. 11, pp. 2417–2430, Nov.  
1105 2010.
- 1106 [10] A. Balenzano, F. Mattia, G. Satalino, and M. W. J. Davidson, "Dense Temporal Series of C- and L-band SAR Data for  
1107 Soil Moisture Retrieval Over Agricultural Crops," *IEEE Journal of Selected Topics in Applied Earth Observations and  
1108 Remote Sensing*, vol. 4, no. 2, pp. 439–450, Jun. 2011.
- 1109 [11] M. A. Karam and A. K. Fung, "Leaf-shape effects in electromagnetic wave scattering from vegetation," *IEEE transactions  
1110 on geoscience and remote sensing*, vol. 27, no. 6, pp. 687–697, 1989.
- 1111 [12] T. Senior, K. Sarabandi, and F. Ulaby, "Measuring and modeling the backscattering cross section of a leaf," *Radio Science*,  
1112 vol. 22, no. 6, pp. 1109–1116, 1987.
- 1113 [13] K. Sarabandi, T. B. Senior, and F. Ulaby, "Effect of curvature on the backscattering from a leaf," *Journal of Electromagnetic  
1114 Waves and Applications*, vol. 2, no. 7, pp. 653–670, 1988.
- 1115 [14] A. McDonald, J. Bennett, G. Cookmartin, S. Crossley, K. Morrison, and S. Quegan, "The effect of leaf geometry on the  
1116 microwave backscatter from leaves," *International Journal of Remote Sensing*, vol. 21, no. 2, pp. 395–400, 2000.
- 1117 [15] D. H. Hoekman and B. A. M. Bouman, "Interpretation of C- and X-band radar images over an agricultural area, the  
1118 Flevoland test site in the Agriscatt-87 campaign," *International Journal of Remote Sensing*, vol. 14, no. 8, pp. 1577–1594,  
1119 May 1993.

- 1120 [16] S. H. Yueh, J. A. Kong, J. K. Jao, R. T. Shin, and T. L. Toan, "Branching model for vegetation," *IEEE Transactions on*  
1121 *Geoscience and Remote Sensing*, vol. 30, no. 2, pp. 390–402, Mar. 1992.
- 1122 [17] M. A. Karam, A. K. Fung, R. H. Lang, and N. S. Chauhan, "A microwave scattering model for layered vegetation," *IEEE*  
1123 *Transactions on Geoscience and Remote Sensing*, vol. 30, no. 4, pp. 767–784, Jul. 1992.
- 1124 [18] F. T. Ulaby and M. A. El-rayes, "Microwave Dielectric Spectrum of Vegetation - Part II: Dual-Dispersion Model," *IEEE*  
1125 *Transactions on Geoscience and Remote Sensing*, vol. GE-25, no. 5, pp. 550–557, Sep. 1987.
- 1126 [19] C. Matzler, "Microwave (1-100 ghz) dielectric model of leaves," *IEEE Transactions on Geoscience and Remote Sensing*,  
1127 vol. 32, no. 4, pp. 947–949, 1994.
- 1128 [20] G. Picard, T. L. Toan, and F. Mattia, "Understanding C-band radar backscatter from wheat canopy using a multiple-  
1129 scattering coherent model," *IEEE Transactions on Geoscience and Remote Sensing*, vol. 41, no. 7, pp. 1583–1591, Jul.  
1130 2003.
- 1131 [21] F. Mattia, T. L. Toan, G. Picard, F. I. Posa, A. D'Alessio, C. Notarnicola, A. M. Gatti, M. Rinaldi, G. Satalino, and  
1132 G. Pasquariello, "Multitemporal C-band radar measurements on wheat fields," *IEEE Transactions on Geoscience and*  
1133 *Remote Sensing*, vol. 41, no. 7, pp. 1551–1560, Jul. 2003.
- 1134 [22] T. L. Toan, F. Ribbes, L.-F. Wang, N. Floury, K.-H. Ding, J. A. Kong, M. Fujita, and T. Kurosu, "Rice crop mapping and  
1135 monitoring using ERS-1 data based on experiment and modeling results," *IEEE Transactions on Geoscience and Remote*  
1136 *Sensing*, vol. 35, no. 1, pp. 41–56, Jan. 1997.
- 1137 [23] X. Blaes, P. Defourny, U. Wegmuller, A. D. Vecchia, L. Guerriero, and P. Ferrazzoli, "C-band polarimetric indexes for  
1138 maize monitoring based on a validated radiative transfer model," *IEEE Transactions on Geoscience and Remote Sensing*,  
1139 vol. 44, no. 4, pp. 791–800, Apr. 2006.
- 1140 [24] J. Casanova, J. Judge, and Miyoung Jang, "Modeling Transmission of Microwaves Through Dynamic Vegetation," *IEEE*  
1141 *Transactions on Geoscience and Remote Sensing*, vol. 45, no. 10, pp. 3145–3149, Oct. 2007.
- 1142 [25] M. S. Moran, P. J. Pinter, B. E. Clothier, and S. G. Allen, "Effect of water stress on the canopy architecture and spectral  
1143 indices of irrigated alfalfa," *Remote sensing of environment*, vol. 29, no. 3, pp. 251–261, 1989. [Online]. Available:  
1144 <http://www.sciencedirect.com/science/article/pii/0034425789900047>
- 1145 [26] D. S. Kimes and J. A. Kirchner, "Diurnal variations of vegetation canopy structure," *International Journal of Remote*  
1146 *Sensing*, vol. 4, no. 2, pp. 257–271, Jan. 1983.
- 1147 [27] T. van Emmerik, S. Steele-Dunne, J. Judge, and N. van de Giesen, "A comparison between leaf dielectric properties of  
1148 stressed and unstressed tomato plants," in *2015 IEEE International Geoscience and Remote Sensing Symposium (IGARSS)*,  
1149 July 2015, pp. 275–278.
- 1150 [28] T. van Emmerik, S. C. Steele-Dunne, J. Judge, and N. van de Giesen, "Impact of Diurnal Variation in Vegetation Water  
1151 Content on Radar Backscatter From Maize During Water Stress," *IEEE Transactions on Geoscience and Remote Sensing*,  
1152 vol. 53, no. 7, pp. 3855–3869, Jul. 2015.
- 1153 [29] T. J. Schmugge, "Remote Sensing of Soil Moisture: Recent Advances," *IEEE Transactions on Geoscience and Remote*  
1154 *Sensing*, vol. GE-21, no. 3, pp. 336–344, Jul. 1983.
- 1155 [30] J. R. Wang, E. T. Engman, T. Mo, T. J. Schmugge, and J. Shiue, "The effects of soil moisture, surface roughness,  
1156 and vegetation on l-band emission and backscatter," *IEEE Transactions on Geoscience and Remote Sensing*, no. 6, pp.  
1157 825–833, 1987.
- 1158 [31] V. Mironov, M. Dobson, V. Kaupp, S. Komarov, and V. Kleshchenko, "Generalized refractive mixing dielectric model  
1159 for moist soils," *IEEE Trans. Geosci. Remote Sensing*, vol. 42, no. 4, pp. 773–785, April 2004.
- 1160 [32] M. C. Dobson, F. T. Ulaby, M. T. Hallikainen, and M. A. El-rayes, "Microwave Dielectric Behavior of Wet Soil-Part II:

- 1161 Dielectric Mixing Models,” *IEEE Transactions on Geoscience and Remote Sensing*, vol. GE-23, no. 1, pp. 35–46, Jan.  
1162 1985.
- 1163 [33] T. F. Bush and F. T. Ulaby, “An evaluation of radar as a crop classifier,” *Remote Sensing of Environment*, vol. 7, no. 1,  
1164 pp. 15–36, Jan. 1978.
- 1165 [34] H. McNairn and B. Brisco, “The application of C-band polarimetric SAR for agriculture: A review,” *Canadian Journal*  
1166 *of Remote Sensing*, vol. 30, no. 3, pp. 525–542, 2004.
- 1167 [35] N. Baghdadi, N. Boyer, P. Todoroff, M. El Hajj, and A. Bgu, “Potential of SAR sensors TerraSAR-X, ASAR/ENVISAT  
1168 and PALSAR/ALOS for monitoring sugarcane crops on Reunion Island,” *Remote Sensing of Environment*, vol. 113, no. 8,  
1169 pp. 1724–1738, Aug. 2009.
- 1170 [36] T. Le Toan, F. Ribbes, L.-F. Wang, N. Floury, K.-H. Ding, J. A. Kong, M. Fujita, and T. Kurosu, “Rice crop mapping and  
1171 monitoring using ERS-1 data based on experiment and modeling results,” *IEEE Transactions on Geoscience and Remote*  
1172 *Sensing*, vol. 35, no. 1, pp. 41–56, 1997.
- 1173 [37] H. Skriver, F. Mattia, G. Satalino, A. Balenzano, V. R. N. Pauwels, N. E. C. Verhoest, and M. Davidson, “Crop  
1174 Classification Using Short-Revisit Multitemporal SAR Data,” *IEEE Journal of Selected Topics in Applied Earth*  
1175 *Observations and Remote Sensing*, vol. 4, no. 2, pp. 423–431, Jun. 2011.
- 1176 [38] G. Macelloni, S. Paloscia, P. Pampaloni, and E. Santi, “Global scale monitoring of soil and vegetation using SSM/I and  
1177 ERS wind scatterometer,” *International Journal of Remote Sensing*, vol. 24, no. 12, pp. 2409–2425, Jan. 2003.
- 1178 [39] L. Jarlan, P. Mazzega, E. Mougin, F. Lavenu, G. Marty, P. Frison, and P. Hiernaux, “Mapping of Sahelian vegetation  
1179 parameters from ERS scatterometer data with an evolution strategies algorithm,” *Remote Sensing of Environment*, vol. 87,  
1180 no. 1, pp. 72–84, Sep. 2003.
- 1181 [40] S. Frolking, T. Milliman, K. McDonald, J. Kimball, M. Zhao, and M. Fahnestock, “Evaluation of the SeaWinds  
1182 scatterometer for regional monitoring of vegetation phenology,” *Journal of Geophysical Research: Atmospheres*, vol.  
1183 111, no. D17, p. D17302, Sep. 2006.
- 1184 [41] P. Frison and E. Mougin, “Monitoring global vegetation dynamics with ERS-1 wind scatterometer data,” *Remote Sensing*,  
1185 vol. 17, no. 16, pp. 3201–3218, 1996.
- 1186 [42] M. Abdel-Messeh and S. Quegan, “Variability in ERS scatterometer measurements over land,” *IEEE transactions on*  
1187 *geoscience and remote sensing*, vol. 38, no. 4, pp. 1767–1776, 2000.
- 1188 [43] P. J. Hardin and M. W. Jackson, “Investigating seawinds terrestrial backscatter,” *Photogrammetric Engineering & Remote*  
1189 *Sensing*, vol. 69, no. 11, pp. 1243–1254, 2003.
- 1190 [44] L. Guerriero, P. Ferrazzoli, and R. Rahmoune, “A synergic view of L-band active and passive remote sensing of vegetated  
1191 soil,” in *2012 12th Specialist Meeting on Microwave Radiometry and Remote Sensing of the Environment (MicroRad)*,  
1192 Mar. 2012, pp. 1–3.
- 1193 [45] D. Entekhabi, E. G. Njoku, P. E. O’Neill, K. H. Kellogg, W. T. Crow, W. N. Edelstein, J. K. Entin, S. D. Goodman, T. J.  
1194 Jackson, J. Johnson, J. Kimball, J. R. Piepmeier, R. D. Koster, N. Martin, K. C. McDonald, M. Moghaddam, S. Moran,  
1195 R. Reichle, J. C. Shi, M. W. Spencer, S. W. Thurman, L. Tsang, and J. Van Zyl, “The Soil Moisture Active Passive  
1196 (SMAP) Mission,” *Proceedings of the IEEE*, vol. 98, no. 5, pp. 704–716, May 2010.
- 1197 [46] R. De Jeu, W. Wagner, T. Holmes, A. Dolman, N. Van De Giesen, and J. Friesen, “Global soil moisture patterns observed  
1198 by space borne microwave radiometers and scatterometers,” *Surveys in Geophysics*, vol. 29, no. 4-5, pp. 399–420, 2008.
- 1199 [47] J. Parajka, V. Naeimi, G. Blöschl, and J. Komma, “Matching ERS scatterometer based soil moisture patterns with  
1200 simulations of a conceptual dual layer hydrologic model over Austria,” *Hydrology and Earth System Sciences*, vol. 13,  
1201 no. 2, pp. 259–271, 2009.

- 1202 [48] S. Schneider, Y. Wang, W. Wagner, and J.-F. Mahfouf, "Impact of ascat soil moisture assimilation on regional precipitation  
1203 forecasts: A case study for austria," *Monthly Weather Review*, vol. 142, no. 4, pp. 1525–1541, 2014.
- 1204 [49] N. Wanders, D. Karssenberg, A. d. Roo, S. De Jong, and M. Bierkens, "The suitability of remotely sensed soil moisture  
1205 for improving operational flood forecasting," *Hydrology and Earth System Sciences*, vol. 18, no. 6, pp. 2343–2357, 2014.
- 1206 [50] F. Ulaby and R. Moore, "Radar sensing of soil moisture," in *1973 Antennas and Propagation Society International  
1207 Symposium*, vol. 11, Apr. 1973, pp. 362–365.
- 1208 [51] F. Ulaby, "Radar measurement of soil moisture content," *IEEE Transactions on Antennas and Propagation*, vol. 22, no. 2,  
1209 pp. 257–265, Mar. 1974.
- 1210 [52] E. P. W. Attema and F. T. Ulaby, "Vegetation modeled as a water cloud," *Radio Science*, vol. 13, no. 2, pp. 357–364,  
1211 Mar. 1978.
- 1212 [53] F. T. Ulaby, A. Aslam, and M. C. Dobson, "Effects of Vegetation Cover on the Radar Sensitivity to Soil Moisture," *IEEE  
1213 Transactions on Geoscience and Remote Sensing*, vol. GE-20, no. 4, pp. 476–481, Oct. 1982.
- 1214 [54] F. Ulaby, "Vegetation clutter model," *IEEE Transactions on Antennas and Propagation*, vol. 28, no. 4, pp. 538–545, Jul.  
1215 1980.
- 1216 [55] F. T. Ulaby and E. A. Wilson, "Microwave Attenuation Properties of Vegetation Canopies," *IEEE Transactions on  
1217 Geoscience and Remote Sensing*, vol. GE-23, no. 5, pp. 746–753, Sep. 1985.
- 1218 [56] A. Tavakoli, K. Sarabandi, and F. T. Ulaby, "Horizontal propagation through periodic vegetation canopies," *IEEE  
1219 Transactions on Antennas and Propagation*, vol. 39, no. 7, pp. 1014–1023, Jul. 1991.
- 1220 [57] G. P. D. Loor, P. Hooeboom, and E. P. W. Attema, "The Dutch ROVE Program," *IEEE Transactions on Geoscience and  
1221 Remote Sensing*, vol. GE-20, no. 1, pp. 3–11, Jan. 1982.
- 1222 [58] L. Krul, "Some results of microwave remote sensing research in The Netherlands with a view to land applications in the  
1223 1990s," *International Journal of Remote Sensing*, vol. 9, no. 10-11, pp. 1553–1563, Oct. 1988.
- 1224 [59] B. A. M. Bouman and H. W. J. van Kasteren, "Ground-based X-band (3-cm wave) radar backscattering of agricultural  
1225 crops. I. Sugar beet and potato; backscattering and crop growth," *Remote Sensing of Environment*, vol. 34, no. 2, pp.  
1226 93–105, Nov. 1990.
- 1227 [60] —, "Ground-based X-band (3-cm wave) radar backscattering of agricultural crops. II. Wheat, barley, and oats; the  
1228 impact of canopy structure," *Remote Sensing of Environment*, vol. 34, no. 2, pp. 107–119, Nov. 1990.
- 1229 [61] B. A. M. Bouman, "Crop parameter estimation from ground-based x-band (3-cm wave) radar backscattering data," *Remote  
1230 Sensing of Environment*, vol. 37, no. 3, pp. 193–205, Sep. 1991.
- 1231 [62] Y. Inoue, T. Kurosu, H. Maeno, S. Uratsuka, T. Kozu, K. Dabrowska-Zielinska, and J. Qi, "Season-long daily measurements  
1232 of multifrequency (ka, ku, x, c, and l) and full-polarization backscatter signatures over paddy rice field and their relationship  
1233 with biological variables," *Remote Sensing of Environment*, vol. 81, no. 2, pp. 194–204, 2002.
- 1234 [63] B. Brisco, R. Brown, J. Gairns, and B. Snider, "Temporal ground-based scatterometer observations of crops in western  
1235 canada," *Canadian Journal of Remote Sensing*, vol. 18, no. 1, pp. 14–21, 1992.
- 1236 [64] B. Brisco, R. Brown, J. Koehler, G. Sofko, and M. Mckibben, "The diurnal pattern of microwave backscattering by  
1237 wheat," *Remote sensing of environment*, vol. 34, no. 1, pp. 37–47, 1990.
- 1238 [65] A. Toure, K. P. B. Thomson, G. Edwards, R. J. Brown, and B. G. Brisco, "Adaptation of the MIMICS backscattering  
1239 model to the agricultural context-wheat and canola at L and C bands," *IEEE Transactions on Geoscience and Remote  
1240 Sensing*, vol. 32, no. 1, pp. 47–61, Jan. 1994.
- 1241 [66] D. Major, A. Smith, M. Hill, W. Willms, B. Brisco, and R. Brown, "Radar backscatter and visible infrared reflectance  
1242 from short-grass prairie," *Canadian Journal of Remote Sensing*, vol. 20, pp. 71–77, 1994.

- 1243 [67] J. Boisvert, Q. Xu, F. Bonn, R. Brown, and A. Fung, "Modelling backscatter in bare organic soils," in *Geoscience*  
1244 *and Remote Sensing Symposium Proceedings, 1998. IGARSS'98. 1998 IEEE International*, vol. 5. IEEE, 1998, pp.  
1245 2366–2368.
- 1246 [68] H. McNairn, J. Boisvert, D. Major, G. Gwyn, R. Brown, and A. Smith, "Identification of agricultural tillage practices  
1247 from c-band radar backscatter," *Canadian Journal of Remote Sensing*, vol. 22, pp. 154–163, 1996.
- 1248 [69] H. McNairn, C. Duguay, J. Boisvert, E. Huffman, and B. Brisco, "Defining the sensitivity of multi-frequency and multi-  
1249 polarized radar backscatter to post-harvest crop residue," *Canadian Journal of Remote Sensing*, vol. 27, pp. 247–263,  
1250 2001.
- 1251 [70] A. Smith and D. Major, "Radar backscatter and crop residues," *Canadian Journal of Remote Sensing*, vol. 22, pp. 243–247,  
1252 1996.
- 1253 [71] B. Brisco, R. Brown, J. Koehler, G. Sofko, J. Koehler, and A. Wacker, "Tillage effects on the radar backscattering  
1254 coefficient of grain stubble fields," *Remote Sensing of Environment*, vol. 34, no. 37-47, 1991.
- 1255 [72] T. Jackson, J. Kimball, A. Colliander, and E. Njoku, "Science calibration and validation plan," 2010.
- 1256 [73] P. E. O'Neill, R. H. Lang, M. Kurum, C. Utku, and K. R. Carver, "Multi-Sensor Microwave Soil Moisture Remote  
1257 Sensing: NASA's Combined Radar/Radiometer (ComRAD) System," in *2006 IEEE MicroRad*, 2006, pp. 50–54.
- 1258 [74] M. Kurum, R. H. Lang, P. E. O'Neill, A. T. Joseph, T. J. Jackson, and M. H. Cosh, "L-Band Radar Estimation of Forest  
1259 Attenuation for Active/Passive Soil Moisture Inversion," *IEEE Transactions on Geoscience and Remote Sensing*, vol. 47,  
1260 no. 9, pp. 3026–3040, Sep. 2009.
- 1261 [75] —, "A First-Order Radiative Transfer Model for Microwave Radiometry of Forest Canopies at L-Band," *IEEE*  
1262 *Transactions on Geoscience and Remote Sensing*, vol. 49, no. 9, pp. 3167–3179, Sep. 2011.
- 1263 [76] P. O'Neill, M. Kurum, A. Joseph, J. Fuchs, P. Young, M. Cosh, and R. Lang, "L-band active / passive time series  
1264 measurements over a growing season using the ComRAD ground-based SMAP simulator," in *2013 IEEE International*  
1265 *Geoscience and Remote Sensing Symposium - IGARSS*, Jul. 2013, pp. 37–40.
- 1266 [77] P. K. Srivastava, P. O'Neill, M. Cosh, R. Lang, and A. Joseph, "Evaluation of radar vegetation indices for vegetation  
1267 water content estimation using data from a ground-based SMAP simulator," in *2015 IEEE International Geoscience and*  
1268 *Remote Sensing Symposium (IGARSS)*, Jul. 2015, pp. 1296–1299.
- 1269 [78] K. Nagarajan, P.-W. Liu, R. DeRoo, J. Judge, R. Akbar, P. Rush, S. Feagle, D. Preston, and R. Terwilleger, "Automated  
1270 L-Band Radar System for Sensing Soil Moisture at High Temporal Resolution," *IEEE Geoscience and Remote Sensing*  
1271 *Letters*, vol. 11, no. 2, pp. 504–508, Feb. 2014.
- 1272 [79] P.-W. Liu, J. Judge, R. D. DeRoo, A. W. England, T. Bongiovanni, and A. Luke, "Dominant backscattering mechanisms at  
1273 L-band during dynamic soil moisture conditions for sandy soils," *Remote Sensing of Environment*, vol. 178, pp. 104–112,  
1274 Jun. 2016.
- 1275 [80] P. W. Liu, J. Judge, R. DeRoo, A. England, and A. Luke, "Utilizing complementarity of active/passive microwave  
1276 observations at L-band for soil moisture studies in sandy soils," in *2013 IEEE International Geoscience and Remote*  
1277 *Sensing Symposium - IGARSS*, Jul. 2013, pp. 743–746.
- 1278 [81] P. W. Liu, J. Judge, R. D. D. Roo, A. W. England, and T. Bongiovanni, "Uncertainty in Soil Moisture Retrievals Using  
1279 the SMAP Combined Active-Passive Algorithm for Growing Sweet Corn," *IEEE Journal of Selected Topics in Applied*  
1280 *Earth Observations and Remote Sensing*, vol. 9, no. 7, pp. 3326–3339, July 2016.
- 1281 [82] A. Monsivais-Huertero, J. Judge, S. Steele-Dunne, and P. W. Liu, "Impact of Bias Correction Methods on Estimation of  
1282 Soil Moisture When Assimilating Active and Passive Microwave Observations," *IEEE Transactions on Geoscience and*  
1283 *Remote Sensing*, vol. 54, no. 1, pp. 262–278, Jan. 2016.

- 1284 [83] J. H. Hwang, S. g. Kwon, and Y. Oh, "Evaluation of calibration accuracy with hps (hongik polarimetric scatterometer)  
1285 system for multi-bands and multi-polarizations," in *Geoscience and Remote Sensing Symposium (IGARSS), 2011 IEEE*  
1286 *International*, July 2011, pp. 3987–3990.
- 1287 [84] Y. Oh and S.-G. Kwon, "Development of a simple scattering model for vegetation canopies and examination of its  
1288 validity with scatterometer measurements of green-onion fields," in *2009 IEEE International Geoscience and Remote*  
1289 *Sensing Symposium*, 2009.
- 1290 [85] S.-G. Kwon, J.-H. Hwang, and Y. Oh, "Soil moisture inversion from X-band SAR and scatterometer data of vegetation  
1291 fields," in *Geoscience and Remote Sensing Symposium (IGARSS), 2011 IEEE International*. IEEE, 2011, pp. 3140–3143.
- 1292 [86] Y. Oh, S.-Y. Hong, Y. Kim, J.-Y. Hong, and Y.-H. Kim, "Polarimetric backscattering coefficients of flooded rice fields at  
1293 L- and C-bands: Measurements, modeling, and data analysis," *IEEE Transactions on Geoscience and Remote Sensing*,  
1294 vol. 47, no. 8, pp. 2714–2721, 2009.
- 1295 [87] S. K. Kweon and Y. Oh, "A modified water-cloud model with leaf angle parameters for microwave backscattering from  
1296 agricultural fields," *IEEE Transactions on Geoscience and Remote Sensing*, vol. 53, no. 5, pp. 2802–2809, May 2015.
- 1297 [88] J. H. Hwang, S. g. Kwon, and Y. Oh, "A rotational high-resolution SAR on a tower at multi-frequencies," in *2012 IEEE*  
1298 *International Geoscience and Remote Sensing Symposium*, July 2012, pp. 6891–6894.
- 1299 [89] P. Snoeij and P. J. Swart, "The DUT airborne scatterometer," *International Journal of Remote Sensing*, vol. 8, no. 11,  
1300 pp. 1709–1716, 1987.
- 1301 [90] R. Bernard, D. Vidal-Madjar, F. Baudin, and G. Laurent, "Data processing and calibration for an airborne scatterometer,"  
1302 *IEEE transactions on geoscience and remote sensing*, no. 5, pp. 709–716, 1986.
- 1303 [91] P. Snoeij, P. Swart, and E. Attema, "The general behavior of the radar signature of different european test sites as  
1304 a function of frequency and polarization," in *Geoscience and Remote Sensing Symposium, 1990. IGARSS'90. Remote*  
1305 *Sensing Science for the Nineties', 10th Annual International*. IEEE, 1990, pp. 2315–2318.
- 1306 [92] B. A. M. Bouman and D. H. Hoekman, "Multi-temporal, multi-frequency radar measurements of agricultural crops during  
1307 the Agriscatt-88 campaign in The Netherlands," *International Journal of Remote Sensing*, vol. 14, no. 8, pp. 1595–1614,  
1308 May 1993.
- 1309 [93] P. Ferrazzoli, S. Paloscia, P. Pampaloni, G. Schiavon, D. Solimini, and P. Coppo, "Sensitivity of microwave measurements  
1310 to vegetation biomass and soil moisture content: a case study," *IEEE Transactions on Geoscience and Remote Sensing*,  
1311 vol. 30, no. 4, pp. 750–756, Jul. 1992.
- 1312 [94] P. Ferrazzoli, S. Paloscia, P. Pampaloni, G. Schiavon, and D. Solimini, "Multisensor, Multifrequency, Multitemporal  
1313 Aircraft Microwave Measurements Over Agricultural Fields," in *Geoscience and Remote Sensing Symposium, 1991.*  
1314 *IGARSS '91. Remote Sensing: Global Monitoring for Earth Management., International*, vol. 4, Jun. 1991, pp. 2261–  
1315 2264.
- 1316 [95] G. Schoups, P. A. Troch, and N. Verhoest, "Soil moisture influences on the radar backscattering of sugar beet fields,"  
1317 *Remote sensing of environment*, vol. 65, no. 2, pp. 184–194, 1998.
- 1318 [96] L. Prevot, I. Champion, and G. Guyot, "Estimating surface soil moisture and leaf area index of a wheat canopy using a  
1319 dual-frequency (C and X bands) scatterometer," *Remote Sensing of Environment*, vol. 46, no. 3, pp. 331–339, Dec. 1993.
- 1320 [97] M. Benallegue, M. Normand, S. Galle, M. Dechambre, O. Taconet, D. Vidal-Madjar, and L. Prevot, "Soil moisture  
1321 assessment at a basin scale using active microwave remote sensing: the agriscatt'88 airborne campaign on the orgeval  
1322 watershed," *REMOTE SENSING*, vol. 15, no. 3, pp. 645–656, 1994.
- 1323 [98] M. Benallegue, O. Taconet, D. Vidal-Madjar, and M. Normand, "The use of radar backscattering signals for measuring  
1324 soil moisture and surface roughness," *Remote Sensing of Environment*, vol. 53, no. 1, pp. 61–68, 1995.

- 1325 [99] B. Brisco and R. Brown, "Multidate SAR/TM Synergism for Crop Classification in Western Canada," *Photogrammetric*  
1326 *Engineering and Remote Sensing*, vol. 61, pp. 1009–1014, 1995.
- 1327 [100] B. Brisco and R. Protz, "Corn field identification accuracy using airborne radar imagery," *Canadian Journal of Remote*  
1328 *Sensing*, vol. 6, pp. 15–24, 1980.
- 1329 [101] R. Raney, *Principles and Applications of Imaging Radar, Manual of Remote Sensing*, 3rd ed. New York: John Wiley &  
1330 Sons, Inc, 1998, vol. 2, book section Radar Fundamentals: Technical Perspective, pp. 9–130.
- 1331 [102] H. McNairn, J. Van der Sanden, R. Brown, and J. Ellis, "The potential of RADARSAT-2 for crop mapping and assessing  
1332 crop condition," in *Second International Conference on Geospatial Information in Agriculture and Forestry, Lake Buena*  
1333 *Vista, FL*, 2000.
- 1334 [103] H. McNairn, V. Decker, and K. Murnaghan, "The sensitivity of C-Band polarimetric SAR to crop condition," 24–28 June  
1335 2002 2002.
- 1336 [104] H. McNairn, K. Hochheim, and N. Rabe, "Applying polarimetric radar imagery for mapping the productivity  
1337 of wheat crops," *Canadian Journal of Remote Sensing*, vol. 30, no. 3, pp. 517–524, 2004. [Online]. Available:  
1338 <http://www.tandfonline.com/doi/abs/10.5589/m03-068>
- 1339 [105] F. Campbell, R. Ryerson, and R. Brown, "Globesar: a canadian radar remote sensing program," *Geocarto International*,  
1340 vol. 10, no. 3, pp. 3–7, 1995.
- 1341 [106] F. Petzinger, "GlobeSAR: The CCRS airborne SAR in the era of RADARSAT," *Geocarto International*, vol. 10, no. 3,  
1342 pp. 9–17, 1995.
- 1343 [107] R. Brown, M. D'Iorio, and B. Brisco, "GlobeSAR applications review," *Geocarto International*, vol. 10, no. 3, pp. 19–31,  
1344 1995.
- 1345 [108] K. Weise and M. W. Davidson, "Dualband-TerraSAR simulation/campaign results for L-band configuration," in *Geoscience*  
1346 *and Remote Sensing Symposium, 2004. IGARSS'04. Proceedings. 2004 IEEE International*, vol. 7. IEEE, 2004, pp.  
1347 4556–4559.
- 1348 [109] G. Satalino, A. Balenzano, F. Mattia, M. Rinaldi, C. Maddaluno, and G. Annicchiarico, "Retrieval of wheat biomass from  
1349 multitemporal dual polarised sar observations," in *2015 IEEE International Geoscience and Remote Sensing Symposium*  
1350 *(IGARSS)*, July 2015, pp. 5194–5197.
- 1351 [110] A. Burini, F. D. Frate, A. Minchella, G. Schiavon, D. Solimini, R. Bianchi, L. Fusco, and R. Horn, "Multi-temporal high-  
1352 resolution polarimetric l-band sar observation of a wine-producing landscape," in *2006 IEEE International Symposium*  
1353 *on Geoscience and Remote Sensing*, July 2006, pp. 501–503.
- 1354 [111] G. Schiavon, D. Solimini, and A. Burini, "Sensitivity of multi-temporal high resolution polarimetric C and L-band SAR to  
1355 grapes in vineyards," in *2007 IEEE International Geoscience and Remote Sensing Symposium*, July 2007, pp. 3651–3654.
- 1356 [112] A. Burini, G. Schiavon, and D. Solimini, "Fusion of High Resolution Polarimetric SAR and Multi-Spectral Optical Data  
1357 for Precision Viticulture," in *IGARSS 2008 - 2008 IEEE International Geoscience and Remote Sensing Symposium*, vol. 3,  
1358 July 2008, pp. III – 1000–III – 1003.
- 1359 [113] R. Scheiber, N. Oppelt, R. Horn, I. Hajnsek, K. Ben Khadhra, M. Keller, S. Wegscheider, W. Mauser, B. Ben Bacchar, and  
1360 R. Bianchi, "Aquiferex optical and radar campaign-objectives and first results," in *Proceedings of European Conference*  
1361 *on Synthetic Aperture Radar (EUSAR)*. VDE Verlag GmbH, Berlin, Offenburg, 2006, p. 4.
- 1362 [114] Z. Su, W. J. Timmermans, C. van der Tol, R. Dost, R. Bianchi, J. A. Gmez, A. House, I. Hajnsek, M. Menenti, V. Magliulo,  
1363 M. Esposito, R. Haarbrink, F. Bosveld, R. Rothe, H. K. Baltink, Z. Vekerdy, J. A. Sobrino, J. Timmermans, P. van Laake,  
1364 S. Salama, H. van der Kwast, E. Claassen, A. Stolk, L. Jia, E. Moors, O. Hartogensis, and A. Gillespie, "EAGLE 2006  
1365 Multi-purpose, multi-angle and multi-sensor in-situ and airborne campaigns over grassland and forest," *Hydrol. Earth*  
1366 *Syst. Sci.*, vol. 13, no. 6, pp. 833–845, Jun. 2009.

- 1367 [115] R. Bianchi, M. Davidson, I. Hajnsek, M. Wooding, and C. Wloczyk, “AgriSAR 2006—esa final report, noordwijk, the  
1368 netherlands,” 2008.
- 1369 [116] I. Hajnsek, R. Bianchi, M. Davidson, G. D’Urso, J. Gomez-Sanchez, A. Hausold, R. Horn, J. Howse, A. Loew, J. Lopez-  
1370 Sanchez *et al.*, “AgriSAR 2006 Airborne SAR and optics campaigns for an improved monitoring of agricultural processes  
1371 and practices,” in *Geophys. Res. Abstr.*, vol. 9, 2007, p. 04085.
- 1372 [117] J. Stamenković, P. Ferrazzoli, L. Guerriero, D. Tuia, and J.-P. Thiran, “Joining a discrete radiative transfer model and a  
1373 kernel retrieval algorithm for soil moisture estimation from sar data,” *IEEE Journal of Selected Topics in Applied Earth  
1374 Observations and Remote Sensing*, vol. 8, no. 7, pp. 3463–3475, 2015.
- 1375 [118] F. Mattia, G. Satalino, V. Pauwels, and A. Loew, “Soil moisture retrieval through a merging of multi-temporal l-band sar  
1376 data and hydrologic modelling,” *Hydrology and Earth System Sciences*, vol. 13, no. 3, pp. 343–356, 2009.
- 1377 [119] W. J. Wilson, S. H. Yueh, S. J. Dinardo, S. L. Chazanoff, A. Kitiyakara, F. K. Li, and Y. Rahmat-Samii, “Passive  
1378 active l-and s-band (pals) microwave sensor for ocean salinity and soil moisture measurements,” *IEEE Transactions on  
1379 Geoscience and Remote Sensing*, vol. 39, no. 5, pp. 1039–1048, 2001.
- 1380 [120] A. Colliander, S. Chan, S.-b. Kim, N. Das, S. Yueh, M. Cosh, R. Bindlish, T. Jackson, and E. Njoku, “Long term  
1381 analysis of pals soil moisture campaign measurements for global soil moisture algorithm development,” *Remote Sensing  
1382 of Environment*, vol. 121, pp. 309–322, 2012.
- 1383 [121] E. G. Njoku, W. J. Wilson, S. H. Yueh, S. J. Dinardo, F. K. Li, T. J. Jackson, V. Lakshmi, and J. Bolten, “Observations  
1384 of soil moisture using a passive and active low-frequency microwave airborne sensor during sgp99,” *IEEE Transactions  
1385 on Geoscience and Remote Sensing*, vol. 40, no. 12, pp. 2659–2673, 2002.
- 1386 [122] U. Narayan, V. Lakshmi, and E. G. Njoku, “Retrieval of soil moisture from passive and active l/s band sensor (pals)  
1387 observations during the soil moisture experiment in 2002 (smex02),” *Remote Sensing of Environment*, vol. 92, no. 4, pp.  
1388 483–496, 2004.
- 1389 [123] A. Colliander, T. Jackson, H. McNairn, S. Chazanoff, S. Dinardo, B. Latham, I. O’Dwyer, W. Chun, S. Yueh, and  
1390 E. Njoku, “Comparison of airborne passive and active l-band system (pals) brightness temperature measurements to smos  
1391 observations during the smap validation experiment 2012 (smapvex12),” *IEEE Geoscience and Remote Sensing Letters*,  
1392 vol. 12, no. 4, pp. 801–805, 2015.
- 1393 [124] H. McNairn, T. J. Jackson, G. Wiseman, S. Belair, A. Berg, P. Bullock, A. Colliander, M. H. Cosh, S.-B. Kim, R. Magagi  
1394 *et al.*, “The soil moisture active passive validation experiment 2012 (smapvex12): Prelaunch calibration and validation of  
1395 the smap soil moisture algorithms,” *IEEE Transactions on Geoscience and Remote Sensing*, vol. 53, no. 5, pp. 2784–2801,  
1396 2015.
- 1397 [125] N. N. Das, D. Entekhabi, E. G. Njoku, J. J. Shi, J. T. Johnson, and A. Colliander, “Tests of the smap combined radar and  
1398 radiometer algorithm using airborne field campaign observations and simulated data,” *IEEE Transactions on Geoscience  
1399 and Remote Sensing*, vol. 52, no. 4, pp. 2018–2028, 2014.
- 1400 [126] M. Piles, D. Entekhabi, and A. Camps, “A change detection algorithm for retrieving high-resolution soil moisture from  
1401 smap radar and radiometer observations,” *IEEE Transactions on Geoscience and Remote Sensing*, vol. 47, no. 12, pp.  
1402 4125–4131, 2009.
- 1403 [127] D. Gray, R. Yang, H. Yardley, J. Walker, B. Bates, R. Panciera, J. Hacker, A. McGrath, and N. Stacy, “Plis: An airborne  
1404 polarimetric l-band interferometric synthetic aperture radar,” in *Synthetic Aperture Radar (AP SAR), 2011 3rd International  
1405 Asia-Pacific Conference on.* IEEE, 2011, pp. 1–4.
- 1406 [128] R. Panciera, J. P. Walker, T. J. Jackson, D. A. Gray, M. A. Tanase, D. Ryu, A. Monerris, H. Yardley, C. Rüdiger, X. Wu  
1407 *et al.*, “The soil moisture active passive experiments (smapex): Toward soil moisture retrieval from the smap mission,”  
1408 *IEEE transactions on geoscience and remote sensing*, vol. 52, no. 1, pp. 490–507, 2014.

- 1409 [129] R. Panciera, M. A. Tanase, K. Lowell, and J. P. Walker, "Evaluation of iem, dubois, and oh radar backscatter models  
1410 using airborne l-band sar," *IEEE Transactions on Geoscience and Remote Sensing*, vol. 52, no. 8, pp. 4966–4979, 2014.
- 1411 [130] X. Wu, J. P. Walker, C. Rüdiger, R. Panciera, and D. A. Gray, "Simulation of the smap data stream from smapex field  
1412 campaigns in australia," *IEEE Transactions on Geoscience and Remote Sensing*, vol. 53, no. 4, pp. 1921–1934, 2015.
- 1413 [131] X. Wu, J. P. Walker, N. N. Das, R. Panciera, and C. Rüdiger, "Evaluation of the smap brightness temperature downscaling  
1414 algorithm using active–passive microwave observations," *Remote Sensing of Environment*, vol. 155, pp. 210–221, 2014.
- 1415 [132] F. Ulaby, R. More, and A. Fung, *Microwave Remote Sensing: Active and Passive. Vol. II.* Boston, MA: Artech House,  
1416 1986.
- 1417 [133] F. Ulaby and C. Elachi, *Radar Polarimetry for Geoscience Applications.* Norwood, MA: Artech House, 1990.
- 1418 [134] H. Lievens and N. Verhoest, "On the retrieval of soil moisture in wheat fields from l-band sar based on water cloud  
1419 modeling, the iem, and effective roughness parameters," *IEEE Geoscience and Remote Sensing Letters*, vol. 8, no. 4, pp.  
1420 740–744, 2011.
- 1421 [135] Y. Inoue, E. Sakaiya, and C. Wang, "Capability of c-band backscattering coefficients from high-resolution satellite sar  
1422 sensors to assess biophysical variables in paddy rice," *Remote Sensing of Environment*, vol. 140, pp. 247–266, 2014.
- 1423 [136] M. Hosseini, H. McNairn, A. Merzouki, and A. Pacheco, "Estimation of leaf area index (lai) in corn and soybeans using  
1424 multi-polarization c- and l-band radar data," *Remote Sensing of Environment*, vol. 170, pp. 77–89, 2015.
- 1425 [137] E. Beriaux, S. Lambot, and P. Defourny, "Estimating surface-soil moisture for retrieving maize leaf-area index from sar  
1426 data," *Canadian Journal of Remote Sensing*, vol. 37, no. 1, pp. 136–150, 2011.
- 1427 [138] R. Bindlish and A. P. Barros, "Parameterization of vegetation backscatter in radar-based, soil moisture estimation," *Remote  
1428 Sensing of Environment*, vol. 76, no. 1, pp. 130–137, 2001.
- 1429 [139] A. Monsivais-Huertero and J. Judge, "Comparison of Backscattering Models at L-Band for Growing Corn," *IEEE  
1430 Geoscience and Remote Sensing Letters*, vol. 8, no. 1, pp. 24–28, Jan. 2011.
- 1431 [140] N. S. Chauhan, R. H. Lang, and K. J. Ranson, "Radar modeling of a boreal forest," *IEEE Transactions on Geoscience  
1432 and Remote Sensing*, vol. 29, no. 4, pp. 627–638, 1991.
- 1433 [141] S. L. Durden, J. J. Van Zyl, and H. A. Zebker, "Modeling and observation of the radar polarization signature of forested  
1434 areas," *IEEE Transactions on Geoscience and Remote Sensing*, vol. 27, no. 3, pp. 290–301, 1989.
- 1435 [142] Y. Wang, J. Day, and G. Sun, "Santa Barbara Microwave Backscatter Canopy Model for woodlands," *Int. J. Remote  
1436 Sensing*, vol. 14, no. 8, pp. 1477–1493, 1993.
- 1437 [143] F. T. Ulaby, K. Sarabandi, K. McDONALD, M. Whitt, and M. C. Dobson, "Michigan microwave canopy scattering  
1438 model," *International Journal of Remote Sensing*, vol. 11, no. 7, pp. 1223–1253, Jul. 1990.
- 1439 [144] Y. Kerr, J. Wigneron *et al.*, "Vegetation models and observations: A review," *Passive Microwave Remote Sensing of  
1440 Land-Atmosphere Interactions*, pp. 317–344, 1995.
- 1441 [145] S. Chandrasekhar, *Radiative transfer.* Courier Corporation, 2013.
- 1442 [146] P. Ferrazzoli and L. Guerriero, "Radar sensitivity to tree geometry and woody volume: a model analysis," *IEEE  
1443 Transactions on Geoscience and Remote Sensing*, vol. 33, pp. 360–371, 1995.
- 1444 [147] L. Tsang, J. Kong, Z. Chen, K. Pak, and C. Hsu, "Theory of microwave scattering from vegetation based on the collective  
1445 scattering effects of discrete scatterers," in *Proceedings of the ESA/NASA International Workshop on Passive Microwave  
1446 Remote Sensing Research Related to Land-Atmosphere Interactions.* VSP The Netherlands, 1995, pp. 117–154.
- 1447 [148] M. Bracaglia, P. Ferrazzoli, and L. Guerriero, "A fully polarimetric multiple scattering model for crops," *Remote Sensing  
1448 of Environment*, vol. 54, no. 3, pp. 170–179, 1995.
- 1449 [149] R. D. d. Roo, Y. Du, F. T. Ulaby, and M. C. Dobson, "A semi-empirical backscattering model at L-band and C-band for

- 1450 a soybean canopy with soil moisture inversion,” *IEEE Transactions on Geoscience and Remote Sensing*, vol. 39, no. 4,  
1451 pp. 864–872, Apr. 2001.
- 1452 [150] P.-W. Liu, T. Bongiovanni, A. Monsivais-Huertero, J. Judge, S. Steele-Dunne, R. Bindlish, and T. J. Jackson, “Assimilation  
1453 of Active and Passive Microwave Observations for Improved Estimates of Soil Moisture and Crop Growth,” *IEEE Journal*  
1454 *of Selected Topics in Applied Earth Observations and Remote Sensing*, vol. 9, no. 4, pp. 1357–1369, Apr. 2016.
- 1455 [151] P. Ferrazzoli, L. Guerriero, and G. Schiavon, “A vegetation classification scheme validated by model simulations,” in  
1456 *Geoscience and Remote Sensing, 1997. IGARSS '97. Remote Sensing - A Scientific Vision for Sustainable Development.,*  
1457 *1997 IEEE International*, vol. 4, Aug. 1997, pp. 1618–1620 vol.4.
- 1458 [152] P. Ferrazzoli, L. Guerriero, and D. Solimini, “Expected performance of a polarimetric bistatic radar for monitoring  
1459 vegetation,” in *Geoscience and Remote Sensing Symposium, 2000. Proceedings. IGARSS 2000. IEEE 2000 International*,  
1460 vol. 3, 2000, pp. 1018–1020 vol.3.
- 1461 [153] P. Ferrazzoli, L. Guerriero, A. Quesney, O. Taconet, and J. P. Wigneron, “Investigating the capability of C-band radar  
1462 to monitor wheat characteristics,” in *Geoscience and Remote Sensing Symposium, 1999. IGARSS '99 Proceedings. IEEE*  
1463 *1999 International*, vol. 2, 1999, pp. 723–725 vol.2.
- 1464 [154] A. D. Vecchia, P. Ferrazzoli, J. P. Wigneron, and J. P. Grant, “Modeling Forest Emissivity at L-Band and a Comparison  
1465 With Multitemporal Measurements,” *IEEE Geoscience and Remote Sensing Letters*, vol. 4, no. 4, pp. 508–512, Oct. 2007.
- 1466 [155] A. D. Vecchia, P. Ferrazzoli, L. Guerriero, X. Blaes, P. Defourny, L. Dente, F. Mattia, G. Satalino, T. Strozzi, and  
1467 U. Wegmuller, “Influence of geometrical factors on crop backscattering at C-band,” *IEEE Transactions on Geoscience*  
1468 *and Remote Sensing*, vol. 44, no. 4, pp. 778–790, Apr. 2006.
- 1469 [156] A. D. Vecchia, P. Ferrazzoli, L. Guerriero, L. Ninivaggi, T. Strozzi, and U. Wegmuller, “Observing and Modeling  
1470 Multifrequency Scattering of Maize During the Whole Growth Cycle,” *IEEE Transactions on Geoscience and Remote*  
1471 *Sensing*, vol. 46, no. 11, pp. 3709–3718, Nov. 2008.
- 1472 [157] L. Thirion, I. Chenerie, and C. Galy, “Application of a coherent model in simulating the backscattering coefficient of a  
1473 mangrove forest,” *Wave Random Media*, vol. 14, no. 2, pp. 393–414, April 2004.
- 1474 [158] J. M. Stiles and K. Sarabandi, “Electromagnetic scattering from grassland. I. A fully phase-coherent scattering model,”  
1475 *IEEE Transactions on Geoscience and Remote Sensing*, vol. 38, no. 1, pp. 339–348, Jan. 2000.
- 1476 [159] J. Stiles and K. Sarabandi, “Electromagnetics scattering from grassland. I. A fully phase-coherent scattering model,” *IEEE*  
1477 *Trans. Geosci. Remote Sensing*, vol. 38, no. 1, pp. 339–348, January 2000.
- 1478 [160] J. Stiles, K. Sarabandi, and F. Ulaby, “Electromagnetics scattering from grassland. II. Measurement and modeling results,”  
1479 *IEEE Trans. Geosci. Remote Sensing*, vol. 38, no. 1, pp. 349–356, January 2000.
- 1480 [161] Y.-C. Lin and K. Sarabandi, “A coherent scattering model for forest canopies based on monte carlo simulation of fractal  
1481 generated trees,” in *Geoscience and Remote Sensing Symposium, 1996. IGARSS'96. Remote Sensing for a Sustainable*  
1482 *Future., International*, vol. 2. IEEE, 1996, pp. 1334–1336.
- 1483 [162] N. S. Chauhan, D. M. L. Vine, and R. H. Lang, “Discrete scatter model for microwave radar and radiometer response to  
1484 corn: comparison of theory and data,” *IEEE Transactions on Geoscience and Remote Sensing*, vol. 32, no. 2, pp. 416–426,  
1485 Mar. 1994.
- 1486 [163] C. Liu, J. Shang, P. Vachon, and H. McNairn, “Multiyear crop monitoring using polarimetric radarsat-2 data,” *IEEE*  
1487 *Transactions on Geoscience and Remote Sensing*, vol. 51, no. 4, pp. 2227–2240, 2013.
- 1488 [164] A. Freeman and S. L. Durden, “A three-component scattering model for polarimetric sar data,” *IEEE Transactions on*  
1489 *Geoscience and Remote Sensing*, vol. 36, no. 3, pp. 963–973, 1998.
- 1490 [165] Y. Yamaguchi, A. Sato, W. Boerner, R. Sato, and H. Yamada, “Four-component scattering power decomposition with  
1491 rotation of coherence matrix,” *IEEE Transactions on Geoscience and Remote Sensing*, vol. 49, pp. 2251–2258, 2011.

- 1492 [166] A. Sato, Y. Yamaguchi, G. Singh, and S.-E. Park, "Four-component scattering power decomposition with extended volume  
1493 scattering model," *IEEE Geoscience and Remote Sensing Letters*, vol. 9, pp. 166–170, 2012.
- 1494 [167] J. Lee and L. Thomas, "The effect of orientation angle compensation on coherency matrix and polarimetric target  
1495 decompositions," *IEEE Transactions on Geoscience and Remote Sensing*, vol. 49, pp. 53–64, 2009.
- 1496 [168] S. Cloude and E. Pottier, "An entropy based classification scheme for land applications of polarimetric sar," *IEEE  
1497 Transactions on Geoscience and Remote Sensing*, vol. 35, pp. 68–78, 1997.
- 1498 [169] V. Alberga, G. Satalino, and D. Staykova, "Comparison of polarimetric sar observables in terms of classification  
1499 performance," *International Journal of Remote Sensing*, vol. 29, no. 14, pp. 4129–4150, 2008.
- 1500 [170] J. Lee and E. Pottier, *Polarimetric Radar Imaging: From Basics to Applications*. New York: CRC Press, 2009.
- 1501 [171] J. M. Lopez-Sanchez, F. Vicente-Guijalba, J. D. Ballester-Berman, and S. R. Cloude, "Polarimetric Response of Rice  
1502 Fields at C-Band: Analysis and Phenology Retrieval," *IEEE Transactions on Geoscience and Remote Sensing*, vol. 52,  
1503 no. 5, pp. 2977–2993, May 2014.
- 1504 [172] J. R. Adams, T. L. Rowlandson, S. J. McKeown, A. A. Berg, H. McNairn, and S. J. Sweeney, "Evaluating the CloudePottier  
1505 and FreemanDurden scattering decompositions for distinguishing between unharvested and post-harvest agricultural fields,"  
1506 *Canadian Journal of Remote Sensing*, vol. 39, no. 4, pp. 318–327, Oct. 2013.
- 1507 [173] I. H. Woodhouse and D. H. Hoekman, "Determining land-surface parameters from the ERS wind scatterometer,"  
1508 *Geoscience and Remote Sensing, IEEE Transactions on*, vol. 38, no. 1, pp. 126–140, 2000.
- 1509 [174] —, "A model-based determination of soil moisture trends in Spain with the ERS-scatterometer," *IEEE Transactions on  
1510 Geoscience and Remote Sensing*, vol. 38, no. 4, pp. 1783–1793, Jul. 2000.
- 1511 [175] P. L. Frison, E. Mougin, L. Jarlan, M. A. Karam, and P. Hiernaux, "Comparison of ers wind-scatterometer and ssm/i  
1512 data for sahelian vegetation monitoring," *IEEE Transactions on Geoscience and Remote Sensing*, vol. 38, no. 4, pp.  
1513 1794–1803, Jul 2000.
- 1514 [176] L. Jarlan, P. Mazzega, and E. Mougin, "Retrieval of land surface parameters in the sahel from ers wind scatterometer  
1515 data: a "brute force" method," *IEEE Transactions on Geoscience and Remote Sensing*, vol. 40, no. 9, pp. 2056–2062,  
1516 Sep 2002.
- 1517 [177] L. Jarlan, P. Mazzega, E. Mougin, F. Lavenu, G. Marty, P. Frison, and P. Hiernaux, "Mapping of sahelian vegetation  
1518 parameters from ers scatterometer data with an evolution strategies algorithm," *Remote Sensing of Environment*, vol. 87,  
1519 no. 1, pp. 72–84, 2003.
- 1520 [178] M. Grippa and I. H. Woodhouse, "Retrieval of bare soil and vegetation parameters from wind scatterometer measurements  
1521 over three different climatic regions," *Remote Sensing of Environment*, vol. 84, no. 1, pp. 16–24, 2003.
- 1522 [179] L. Lu, H. Guo, C. Wang, and Q. Li, "Assessment of the seawinds scatterometer for vegetation phenology monitoring  
1523 across china," *International journal of remote sensing*, vol. 34, no. 15, pp. 5551–5568, 2013.
- 1524 [180] N. Ringelmann, K. Scipal, Z. Bartalis, and W. Wagner, "Planting date estimation in semi-arid environments based on  
1525 ku-band radar scatterometer data," in *Geoscience and Remote Sensing Symposium, 2004. IGARSS '04. Proceedings. 2004  
1526 IEEE International*, vol. 2, Sept 2004, pp. 1288–1291.
- 1527 [181] P. J. Hardin and M. W. Jackson, "Examining vegetation phenological change in south america using reconstructed  
1528 seawinds data: grasslands and savanna," in *Geoscience and Remote Sensing Symposium, 2002. IGARSS '02. 2002 IEEE  
1529 International*, vol. 6, 2002, pp. 3296–3298 vol.6.
- 1530 [182] T. L. Toan, F. Ribbes, L.-F. Wang, N. Floury, K.-H. Ding, J. A. Kong, M. Fujita, and T. Kurosu, "Rice crop mapping and  
1531 monitoring using ERS-I data based on experiment and modeling results," *IEEE Transactions on Geoscience and Remote  
1532 Sensing*, vol. 35, no. 1, pp. 41–56, Jan 1997.

- 1533 [183] F. Ribbes, "Rice field mapping and monitoring with radarsat data," *International Journal of Remote Sensing*, vol. 20,  
1534 no. 4, pp. 745–765, 1999.
- 1535 [184] A. Bouvet, T. L. Toan, and N. L. Dao, "Estimation of agricultural and biophysical parameters of rice fields in vietnam  
1536 using x-band dual-polarization sar," in *2014 IEEE Geoscience and Remote Sensing Symposium*, July 2014, pp. 1504–1507.
- 1537 [185] H. McNairn, A. Kross, D. Lapen, R. Caves, and J. Shang, "Early Season Monitoring of Corn and Soybeans with TerraSAR-  
1538 X and RADARSAT-2," *International Journal of Applied Earth Observation and Geoinformation*, vol. 28, pp. 252–259,  
1539 2014.
- 1540 [186] H. McNairn, J. Shang, X. Jiao, and C. Champagne, "The contribution of alos palsar multipolarization and polarimetric  
1541 data to crop classification," *IEEE Transactions on Geoscience and Remote Sensing*, vol. 47, pp. 3981–3992, 2009.
- 1542 [187] B. Deschamps, H. McNairn, J. Shang, and X. Jiao, "Towards operational radar-only crop type classification: comparison  
1543 of a traditional decision tree with a random forest classifier," *Canadian Journal of Remote Sensing*, vol. 38, no. 1, pp.  
1544 60–68, 2012.
- 1545 [188] C. Chen and H. McNairn, "A neural network integrated approach for rice crop monitoring," *International Journal of  
1546 Remote Sensing*, vol. 27, no. 7, pp. 1367–1393, 2006.
- 1547 [189] Y. Zhang, C. Wang, J. Wu, J. Qi, and W. A. Salas, "Mapping paddy rice with multitemporal ALOS/PALSAR imagery  
1548 in southeast China," *International Journal of Remote Sensing*, vol. 30, no. 23, pp. 6301–6315, 2009.
- 1549 [190] S. C. Liew, S.-P. Kam, T.-P. Tuong, P. Chen, V. Q. Minh, and H. Lim, "Application of multitemporal ERS-2 synthetic  
1550 aperture radar in delineating rice cropping systems in the Mekong River Delta, Vietnam," *IEEE Transactions on Geoscience  
1551 and Remote Sensing*, vol. 36, no. 5, pp. 1412–1420, 1998.
- 1552 [191] K. Jia, Q. Li, Y. Tian, B. Wu, F. Zhang, and J. Meng, "Crop classification using multi-configuration SAR data in the  
1553 North China Plain," *International Journal of Remote Sensing*, vol. 33, pp. 170–183, 2012.
- 1554 [192] H. Skriver, "Crop Classification by Multitemporal C- and L-Band Single- and Dual-Polarization and Fully Polarimetric  
1555 SAR," *IEEE Transactions on Geoscience and Remote Sensing*, vol. 50, pp. 2138–2149, 2012.
- 1556 [193] M. C. Dobson, L. E. Pierce, and F. T. Ulaby, "Knowledge-based land-cover classification using ERS-1/JERS-1 SAR  
1557 composites," *IEEE Transactions on Geoscience and Remote Sensing*, vol. 34, no. 1, pp. 83–99, 1996.
- 1558 [194] K. Chen, W. Huang, D. Tsay, and F. Amar, "Classification of multifrequency polarimetric SAR imagery using a dynamic  
1559 learning neural network," *IEEE Transactions on Geoscience and Remote Sensing*, vol. 34, no. 3, pp. 814–820, 1996.
- 1560 [195] P. Ferrazzoli, S. Paloscia, P. Pampaloni, G. Schiavon, S. Sigismondi, and D. Solimini, "The potential of multifrequency  
1561 polarimetric SAR in assessing agricultural and arboreous biomass," *IEEE Transactions on Geoscience and Remote Sensing*,  
1562 vol. 35, no. 1, pp. 5–17, Jan. 1997.
- 1563 [196] P. Ferrazzoli, L. Guerriero, and G. Schiavon, "Experimental and model investigation on radar classification capability,"  
1564 *IEEE Transactions on Geoscience and Remote Sensing*, vol. 37, no. 2, pp. 960–968, Mar. 1999.
- 1565 [197] M. Hill, C. Ticehurst, J.-S. Lee, M. Grunes, G. Donald, and D. Henry, "Integration of Optical and Radar Classifications  
1566 for Mapping Pasture Type in Western Australia," *IEEE Transactions on Geoscience and Remote Sensing*, vol. 43, no.  
1567 1665–1681, 2005.
- 1568 [198] D. H. Hoekman, M. A. M. Vissers, and T. N. Tran, "Unsupervised Full-Polarimetric SAR Data Segmentation as a Tool  
1569 for Classification of Agricultural Areas," *IEEE Journal of Selected Topics in Applied Earth Observations and Remote  
1570 Sensing*, vol. 4, no. 2, pp. 402–411, Jun. 2011.
- 1571 [199] G. Foody, M. McCulloch, and W. Yates, "Crop classification from C-band polarimetric radar data," *International Journal  
1572 of Remote Sensing*, vol. 15, no. 14, pp. 2871–2885, 1994.
- 1573 [200] J.-S. Lee, M. Grunes, and E. Pottier, "Quantitative comparison of classification capability: Fully polarimetric versus dual

- 1574 and single-polarization SAR,” *IEEE Transactions on Geoscience and Remote Sensing*, vol. 39, no. 11, pp. 2343–2351,  
1575 2001, read.
- 1576 [201] H. McNairn, C. Champagne, J. Shang, D. Holmstrom, and G. Reichert, “Integration of optical and synthetic aperture  
1577 radar (SAR) imagery for delivering operational annual crop inventories,” *ISPRS Journal of Photogrammetry and Remote  
1578 Sensing*, vol. 64, pp. 434–449, 2009.
- 1579 [202] T. Fiset, P. Rollin, Z. Aly, L. Campbell, B. Daneshfar, F. P., A. Smith, A. Davidson, J. Shang, and I. Jarvis, “AAFC  
1580 annual crop inventory: Status and challenges,” 12 - 16 August 2013 2013.
- 1581 [203] D. Hoekman and A. Vissers, “A new polarimetric classification approach evaluated for agricultural crops,” *IEEE  
1582 Transactions on Geoscience and Remote Sensing*, vol. 41, pp. 2881–2889, 2003.
- 1583 [204] F. Charbonneau, B. Brisco, R. Raney, H. McNairn, C. Liu, P. Vachon, J. Shang, C. Champagne, A. Merzouki, and  
1584 T. Geldsetzer, “Compact polarimetry overview and applications assessment,” *Canadian Journal of Remote Sensing*, vol. 36,  
1585 no. 2, pp. 298–315, 2010.
- 1586 [205] A. Chipanshi, Y. Zhang, L. Kouadio, N. Newlands, A. Davidson, H. Hill, R. Warren, B. Qian, B. Daneshfar, F. Bedard,  
1587 and G. Reichert, “Evaluation of the Integrated Canadian Crop Yield Forecaster (ICCYF) model for in-season prediction  
1588 of crop yield across the Canadian agricultural landscape,” *Agricultural and Forest Meteorology*, vol. 206, pp. 137–150,  
1589 2015.
- 1590 [206] J. Liu, E. Pattey, J. Miller, H. McNairn, and A. Smith, “Estimating crop stresses, aboveground dry biomass and yield of  
1591 corn using multi-temporal optical data combined with a radiation use efficiency model,” *Remote Sensing of Environment*,  
1592 vol. 114, no. 6, pp. 1167–1177, 2010.
- 1593 [207] F. Ulaby, C. Allen, G. Eger III, and E. Kanemasu, “Relating the microwave backscattering coefficient to leaf area index,”  
1594 *Remote Sensing of Environment*, vol. 14, pp. 113–133, 1984.
- 1595 [208] J. F. Paris, “Probing Thick Vegetation Canopies with a Field Microwave Scatterometer,” *IEEE Transactions on Geoscience  
1596 and Remote Sensing*, vol. GE-24, no. 6, pp. 886–893, Nov. 1986.
- 1597 [209] H. McNairn, J. Shang, X. Jiao, and B. Deschamps, “Establishing crop productivity using RADARSAT-2, international  
1598 archives of the photogrammetry, remote sensing and spatial information sciences,” 25 August – 01 September 2012 2012.
- 1599 [210] X. Jiao, H. McNairn, J. Shang, E. Pattey, J. Liu, and C. Champagne, “The sensitivity of RADARSAT-2 polarimetric SAR  
1600 data to corn and soybean Leaf Area Index,” *Canadian Journal of Remote Sensing*, vol. 37, no. 1, pp. 69–81, 2011.
- 1601 [211] S. Maity, C. Patnaik, M. Chakraborty, and S. Panigrahy, “Analysis of temporal backscattering of cotton crops using a  
1602 semiempirical model,” *IEEE Transactions on Geoscience and Remote Sensing*, vol. 42, no. 3, pp. 577–587, Mar. 2004.
- 1603 [212] R. Prasad, “Estimation of kidney bean crop variables using ground-based scatterometer data at 9.89 GHz,” *International  
1604 Journal of Remote Sensing*, vol. 32, pp. 31–48, 2011.
- 1605 [213] Y. Kim, T. Jackson, R. Bindlish, H. Lee, and S. Hong, “Monitoring soybean growth using L-, C-, and X-band scatterometer  
1606 data,” *International Journal of Remote Sensing*, vol. 34, no. 11, pp. 4069–4082, Jun. 2013.
- 1607 [214] G. Wiseman, H. McNairn, S. Homayouni, and J. Shang, “RADARSAT-2 Polarimetric SAR Response to Crop Biomass  
1608 for Agricultural Production Monitoring,” *IEEE Journal of Selected Topics in Applied Earth Observations and Remote  
1609 Sensing*, vol. 7, no. 11, pp. 4461–4471, Nov. 2014.
- 1610 [215] S. Paloscia, “A summary of experimental results to assess the contribution of SAR for mapping vegetation biomass and  
1611 soil moisture,” *Canadian Journal of Remote Sensing*, vol. 28, no. 2, pp. 246–261, 2002, not read yet.
- 1612 [216] M. Moran, J. Moreno, M. Mateo, D. de la Cruz, and A. Montoro, “A RADARSAT-2 quad- polarized time series for  
1613 monitoring crop and soil conditions in Barrax, Spain,” *IEEE Transactions on Geoscience and Remote Sensing*, vol. 50,  
1614 pp. 1057–1070, 2012.

- 1615 [217] G. Satalino, L. Dente, and F. Mattia, "Integration of MERIS and ASAR Data for LAI Estimation of Wheat Fields," pp.  
1616 2255–2258, July 31 - August 4 2006.
- 1617 [218] J. Chen, H. Lin, C. Huang, and C. Fang, "The relationship between the leaf area index (LAI) of rice and the Cband SAR  
1618 vertical/horizontal (VV/HH) polarization ratio," *International Journal of Remote Sensing*, vol. 30, no. 8, pp. 2149–2154,  
1619 Apr. 2009.
- 1620 [219] H. Lin, J. Chen, Z. Pei, S. Zhang, and X. Hu, "Monitoring sugarcane growth using ENVISAT ASAR data," *IEEE*  
1621 *Transactions on Geoscience and Remote Sensing*, vol. 47, no. 8, pp. 2572–2580, 2009.
- 1622 [220] Y. Kim and J. J. van Zyl, "A time-series approach to estimate soil moisture using polarimetric radar data," *IEEE*  
1623 *Transactions on Geoscience and Remote Sensing*, vol. 47, no. 8, pp. 2519–2527, 2009.
- 1624 [221] J. Shang, X. Jiao, H. McNairn, J. Kovacs, D. Walters, B. Ma, and X. Geng, "Tracking crop phenological development  
1625 of spring wheat using synthetic aperture radar (sar) in northern ontario, canada," in *Agro-Geoinformatics (Agro-  
1626 Geoinformatics), 2013 Second International Conference on*, Aug 2013, pp. 517–521.
- 1627 [222] J. Shang, E. Huffman, J. Liu, B. Ma, T. Zhao, B. Qian, H. McNairn, X. Geng, and N. Lantz, "Using earth observation  
1628 to monitor corn growth in eastern ontario," 13-14 February 2014 2014.
- 1629 [223] Y. Kim, T. Jackson, R. Bindlish, H. Lee, and S. Hong, "Radar Vegetation Index for Estimating the Vegetation Water  
1630 Content of Rice and Soybean," *IEEE Geoscience and Remote Sensing Letters*, vol. 9, no. 4, pp. 564–568, Jul. 2012.
- 1631 [224] P. Narvekar, D. Entekhabi, S.-B. Kim, and E. Njoku, "Soil moisture retrieval using L-band radar observations," *IEEE*  
1632 *Transactions on Geoscience and Remote Sensing*, vol. 53, no. 6, pp. 3492–3506, 2015.
- 1633 [225] A. Kross, H. McNairn, D. Lapen, M. Sunohara, and C. Champagne, "Assessment of RapidEye vegetation indices for  
1634 estimation of leaf area index and biomass in corn and soybean crops," *International Journal of Applied Earth Observation  
1635 and Geoinformation*, vol. 34, pp. 235–248, 2015.
- 1636 [226] J. M. Lopez-Sanchez, J. D. Ballester-Berman, and I. Hajnsek, "First results of rice monitoring practices in spain by  
1637 means of time series of TerraSAR-X dual-pol images," *IEEE Journal of Selected Topics in Applied Earth Observations  
1638 and Remote Sensing*, vol. 4, no. 2, pp. 412–422, June 2011.
- 1639 [227] J. M. Lopez-Sanchez, S. R. Cloude, and J. D. Ballester-Berman, "Rice phenology monitoring by means of SAR polarimetry  
1640 at X-Band," *IEEE Transactions on Geoscience and Remote Sensing*, vol. 50, no. 7, pp. 2695–2709, July 2012.
- 1641 [228] J. M. Lopez-Sanchez, F. Vicente-Guijalba, J. D. Ballester-Berman, and S. R. Cloude, "Polarimetric response of rice fields  
1642 at C-band: Analysis and phenology retrieval," *IEEE Transactions on Geoscience and Remote Sensing*, vol. 52, no. 5, pp.  
1643 2977–2993, 2014.
- 1644 [229] Z. Yang, K. Li, L. Liu, Y. Shao, B. Brisco, and W. Li, "Rice growth monitoring using simulated compact polarimetric C  
1645 band SAR," *Radio Science*, vol. 49, no. 12, pp. 1300–1315, 2014.
- 1646 [230] Y. Shao, X. Fan, H. Liu, J. Xiao, S. Ross, B. Brisco, R. Brown, and G. Staples, "Rice monitoring and production  
1647 estimation using multitemporal RADARSAT," *Remote sensing of Environment*, vol. 76, no. 3, pp. 310–325, 2001.
- 1648 [231] O. Yuzugullu, E. Erten, and I. Hajnsek, "Rice growth monitoring by means of X-band co-polar SAR: Feature clustering  
1649 and BBCH scale," *IEEE Geoscience and Remote Sensing Letters*, vol. 12, no. 6, pp. 1218–1222, 2015.
- 1650 [232] L. Mascolo, J. Lopez-Sanchez, F. Vicente-Guijalba, G. Mazzarella, F. Nunziata, and M. Migliaccio, "Retrieval of  
1651 phenological stages of onion fields during the first year of growth by means of C-band polarimetric SAR measurements,"  
1652 *International Journal of Remote Sensing*, vol. 36, no. 12, pp. 3077–3096, 2015.
- 1653 [233] F. Nunziata, M. Migliaccio, J. M. L. Sanchez, L. Mascolo, G. Mazzarella, and G. D'Urso, "C-band polarimetric SAR  
1654 measurements for the monitoring of growth stages of corn fields in the piana DEL sele zone," in *2015 IEEE International  
1655 Geoscience and Remote Sensing Symposium (IGARSS)*, July 2015, pp. 3377–3380.

- 1656 [234] L. Zhao, J. Yang, P. Li, and L. Zhang, "Characteristics analysis and classification of crop harvest patterns by exploiting  
1657 high-frequency multipolarization SAR data," *IEEE Journal of Selected Topics in Applied Earth Observations and Remote  
1658 Sensing*, vol. 7, no. 9, pp. 3773–3783, Sept 2014.
- 1659 [235] F. Vicente-Guijalba, T. Martinez-Marin, and J. M. Lopez-Sanchez, "Dynamical approach for real-time monitoring of  
1660 agricultural crops," *IEEE Transactions on Geoscience and Remote Sensing*, vol. 53, no. 6, pp. 3278–3293, June 2015.
- 1661 [236] C. D. Bernardis, F. Vicente-Guijalba, T. Martinez-Marin, and J. M. Lopez-Sanchez, "Contribution to real-time estimation  
1662 of crop phenological states in a dynamical framework based on ndvi time series: Data fusion with sar and temperature,"  
1663 *IEEE Journal of Selected Topics in Applied Earth Observations and Remote Sensing*, vol. 9, no. 8, pp. 3512–3523, Aug  
1664 2016.
- 1665 [237] C. G. De Bernardis, F. Vicente-Guijalba, T. Martinez-Marin, and J. M. Lopez-Sanchez, "Estimation of key dates and  
1666 stages in rice crops using dual-polarization SAR time series and a particle filtering approach," *IEEE Journal of Selected  
1667 Topics in Applied Earth Observations and Remote Sensing*, vol. 8, no. 3, pp. 1008–1018, 2015.
- 1668 [238] F. Vicente-Guijalba, T. Martinez-Marin, and J. M. Lopez-Sanchez, "Crop phenology estimation using a multitemporal  
1669 model and a Kalman filtering strategy," *IEEE Geoscience and Remote Sensing Letters*, vol. 11, no. 6, pp. 1081–1085,  
1670 2014.
- 1671 [239] L. Mascolo, J. M. Lopez-Sanchez, F. Vicente-Guijalba, F. Nunziata, M. Migliaccio, and G. Mazzarella, "A complete  
1672 procedure for crop phenology estimation with PolSAR data based on the Complex Wishart Classifier," *IEEE Transactions  
1673 on Geoscience and Remote Sensing*, vol. 54, no. 11, pp. 6505–6515, Nov 2016.
- 1674 [240] J. M. Lopez-Sanchez and J. D. Ballester-Berman, "Potentials of polarimetric SAR interferometry for agriculture  
1675 monitoring," *Radio Science*, vol. 44, no. 2, p. RS2010, Apr. 2009.
- 1676 [241] A. Ceballos, K. Scipal, W. Wagner, and J. Martinez-Fernandez, "Validation of ERS scatterometer-derived soil moisture  
1677 data in the central part of the Duero Basin, Spain," *Hydrological Processes*, vol. 19, no. 8, pp. 1549–1566, May 2005.  
1678 [Online]. Available: <http://onlinelibrary.wiley.com/doi/10.1002/hyp.5585/abstract>
- 1679 [242] J. D. Bolten, W. T. Crow, X. Zhan, T. J. Jackson, and C. A. Reynolds, "Evaluating the utility of remotely sensed soil  
1680 moisture retrievals for operational agricultural drought monitoring," *IEEE Journal of Selected Topics in Applied Earth  
1681 Observations and Remote Sensing*, vol. 3, no. 1, pp. 57–66, March 2010.
- 1682 [243] W. Wagner, K. Scipal, H. Boogard, K. v. Diepen, R. Beck, E. Nobbe, and I. Savin, "Assessing water-limited crop  
1683 production with a scatterometer based crop growth monitoring system," in *Geoscience and Remote Sensing Symposium,  
1684 2000. Proceedings. IGARSS 2000. IEEE 2000 International*, vol. 4, 2000, pp. 1696–1698 vol.4.
- 1685 [244] A. d. De Wit and C. Van Diepen, "Crop model data assimilation with the ensemble Kalman filter for improving regional  
1686 crop yield forecasts," *Agricultural and Forest Meteorology*, vol. 146, no. 1, pp. 38–56, 2007.
- 1687 [245] S. Chakrabarti, T. Bongiovanni, J. Judge, L. Zotarelli, and C. Bayer, "Assimilation of SMOS soil moisture for quantifying  
1688 drought impacts on crop yield in agricultural regions," *IEEE Journal of Selected Topics in Applied Earth Observations  
1689 and Remote Sensing*, vol. 7, no. 9, pp. 3867–3879, Sept 2014.
- 1690 [246] W. Wagner, S. Hahn, R. Kidd, T. Melzer, Z. Bartalis, S. Hasenauer, J. Figa-Saldae, P. de Rosnay, A. Jann, S. Schneider,  
1691 J. Komma, G. Kubu, K. Brugger, C. Aubrecht, J. Zger, U. Gangkofner, S. Kienberger, L. Brocca, Y. Wang, G. Blschl,  
1692 J. Eitzinger, K. Steinnocher, P. Zeil, and F. Rubel, "The ASCAT Soil Moisture Product: A Review of its Specifications,  
1693 Validation Results, and Emerging Applications," *Meteorologische Zeitschrift*, vol. 22, no. 1, pp. 5–33, Feb. 2013.
- 1694 [247] W. Wagner, G. Lemoine, M. Borgeaud, and H. Rott, "A study of vegetation cover effects on ERS scatterometer data,"  
1695 *IEEE Transactions on Geoscience and Remote Sensing*, vol. 37, no. 2, pp. 938–948, Mar. 1999.
- 1696 [248] W. Wagner, G. Lemoine, and H. Rott, "A method for estimating soil moisture from ERS scatterometer and soil data,"  
1697 *Remote sensing of environment*, vol. 70, no. 2, pp. 191–207, 1999.

- 1698 [249] W. Wagner and K. Scipal, "Large-scale soil moisture mapping in western Africa using the ERS scatterometer," *IEEE*  
1699 *Transactions on Geoscience and Remote Sensing*, vol. 38, no. 4, pp. 1777–1782, Jul. 2000.
- 1700 [250] W. Wagner, K. Scipal, C. Pathe, D. Gerten, W. Lucht, and B. Rudolf, "Evaluation of the agreement between the first global  
1701 remotely sensed soil moisture data with model and precipitation data," *Journal of Geophysical Research: Atmospheres*,  
1702 vol. 108, no. D19, p. 4611, Oct. 2003.
- 1703 [251] Z. Bartalis, W. Wagner, V. Naeimi, S. Hasenauer, K. Scipal, H. Bonekamp, J. Figa, and C. Anderson, "Initial soil moisture  
1704 retrievals from the METOP-A Advanced Scatterometer (ASCAT)," *Geophysical Research Letters*, vol. 34, no. 20, p.  
1705 L20401, Oct. 2007.
- 1706 [252] V. Naeimi, K. Scipal, Z. Bartalis, S. Hasenauer, and W. Wagner, "An Improved Soil Moisture Retrieval Algorithm for  
1707 ERS and METOP Scatterometer Observations," *IEEE Transactions on Geoscience and Remote Sensing*, vol. 47, no. 7,  
1708 pp. 1999–2013, Jul. 2009.
- 1709 [253] W. Dorigo, A. Gruber, R. De Jeu, W. Wagner, T. Stacke, A. Loew, C. Albergel, L. Brocca, D. Chung, R. Parinussa,  
1710 and R. Kidd, "Evaluation of the ESA CCI soil moisture product using ground-based observations," *Remote Sensing of*  
1711 *Environment*, vol. 162, pp. 380–395, Jun. 2015.
- 1712 [254] M. Vreugdenhil, W. A. Dorigo, W. Wagner, R. A. M. d. Jeu, S. Hahn, and M. J. E. v. Marle, "Analyzing the Vegetation  
1713 Parameterization in the TU-Wien ASCAT Soil Moisture Retrieval," *IEEE Transactions on Geoscience and Remote Sensing*,  
1714 vol. 54, no. 6, pp. 3513–3531, Jun. 2016.
- 1715 [255] S.-B. Kim, L. Tsang, J. T. Johnson, S. Huang, J. J. van Zyl, and E. G. Njoku, "Soil Moisture Retrieval Using Time-Series  
1716 Radar Observations Over Bare Surfaces," *IEEE Transactions on Geoscience and Remote Sensing*, vol. 50, no. 5, pp.  
1717 1853–1863, May 2012.
- 1718 [256] S.-B. Kim, M. Moghaddam, L. Tsang, M. Burgin, X. Xu, and E. G. Njoku, "Models of L-Band Radar Backscattering  
1719 Coefficients Over Global Terrain for Soil Moisture Retrieval," *IEEE Transactions on Geoscience and Remote Sensing*,  
1720 vol. 52, no. 2, pp. 1381–1396, Feb. 2014.
- 1721 [257] Yunjin Kim and J. van Zyl, "A Time-Series Approach to Estimate Soil Moisture Using Polarimetric Radar Data," *IEEE*  
1722 *Transactions on Geoscience and Remote Sensing*, vol. 47, no. 8, pp. 2519–2527, Aug. 2009.
- 1723 [258] D. G. Long and P. J. Hardin, "Vegetation studies of the Amazon basin using enhanced resolution Seasat scatterometer  
1724 data," *IEEE Transactions on Geoscience and Remote Sensing*, vol. 32, no. 2, pp. 449–460, Mar. 1994.
- 1725 [259] D. G. Long, P. J. Hardin, and P. T. Whiting, "Resolution enhancement of spaceborne scatterometer data," *IEEE*  
1726 *Transactions on Geoscience and Remote Sensing*, vol. 31, no. 3, pp. 700–715, May 1993.
- 1727 [260] J.-F. Mahfouf, "Assimilation of satellite-derived soil moisture from ASCAT in a limited-area NWP model," *Quarterly*  
1728 *Journal of the Royal Meteorological Society*, vol. 136, no. 648, pp. 784–798, Apr. 2010.
- 1729 [261] K. Scipal, M. Drusch, and W. Wagner, "Assimilation of a ERS scatterometer derived soil moisture index in the ECMWF  
1730 numerical weather prediction system," *Advances in water resources*, vol. 31, no. 8, pp. 1101–1112, 2008.
- 1731 [262] V. R. Pauwels, R. Hoeben, N. E. Verhoest, F. P. De Troch, and P. A. Troch, "Improvement of TOPLATS-based discharge  
1732 predictions through assimilation of ERS-based remotely sensed soil moisture values," *Hydrological Processes*, vol. 16,  
1733 no. 5, pp. 995–1013, 2002.
- 1734 [263] W. Wagner, C. Pathe, M. Doubkova, D. Sabel, A. Bartsch, S. Hasenauer, G. Blschl, K. Scipal, J. Martnez-Fernndez, and  
1735 A. Lw, "Temporal Stability of Soil Moisture and Radar Backscatter Observed by the Advanced Synthetic Aperture Radar  
1736 (ASAR)," *Sensors*, vol. 8, no. 2, pp. 1174–1197, Feb. 2008.
- 1737 [264] J. C. Friesen, *Regional vegetation water effects on satellite soil moisture estimations for West Africa*. TU Delft, Delft  
1738 University of Technology, 2008.

- 1739 [265] S. C. Steele-Dunne, J. Friesen, and N. van de Giesen, "Using Diurnal Variation in Backscatter to Detect Vegetation Water  
1740 Stress," *IEEE Transactions on Geoscience and Remote Sensing*, vol. 50, no. 7, pp. 2618–2629, Jul. 2012.
- 1741 [266] I. Birrer, E. Bracalente, G. Dome, J. Sweet, and G. Berthold, " $\sigma^0$  signature of the Amazon rain forest obtained from the  
1742 Seasat scatterometer," *IEEE Transactions on geoscience and remote sensing*, no. 1, pp. 11–17, 1982.
- 1743 [267] M. Satake and H. Hanado, "Diurnal change of Amazon rain forest  $\sigma^0$  observed by Ku-band spaceborne radar," *IEEE  
1744 Transactions on Geoscience and Remote Sensing*, vol. 42, no. 6, pp. 1127–1134, Jun. 2004.
- 1745 [268] S. Jaruwatanadilok and B. W. Stiles, "Trends and variation in Ku-band backscatter of natural targets on land observed in  
1746 QuikSCAT data," *IEEE Transactions on Geoscience and Remote Sensing*, vol. 52, no. 7, pp. 4383–4390, 2014.
- 1747 [269] F. Ulaby and P. Batlivala, "Diurnal variations of radar backscatter from a vegetation canopy," *IEEE Transactions on  
1748 Antennas and Propagation*, vol. 24, no. 1, pp. 11–17, Jan. 1976.
- 1749 [270] R. Schroeder, K. C. McDonald, M. Azarderakhsh, and R. Zimmermann, "ASCAT MetOp-A diurnal backscatter  
1750 observations of recent vegetation drought patterns over the contiguous U.S.: An assessment of spatial extent and  
1751 relationship with precipitation and crop yield," *Remote Sensing of Environment*, vol. 177, pp. 153–159, May 2016.
- 1752 [271] W. Wagner, S. Hahn, R. Kidd, T. Melzer, Z. Bartalis, S. Hasenauer, J. Figa-Saldaña, P. de Rosnay, A. Jann, S. Schneider  
1753 *et al.*, "The ASCAT soil moisture product: A review of its specifications, validation results, and emerging applications,"  
1754 *Meteorologische Zeitschrift*, vol. 22, no. 1, pp. 5–33, 2013.
- 1755 [272] J. Way, J. Paris, M. Dobson, K. McDons, F. Ulaby, J. Weber, L. Ustin, V. Vanderbilt, and E. Kasischke, "Diurnal change  
1756 in trees as observed by optical and microwave sensors: the EOS synergism study," *IEEE Transactions on Geoscience and  
1757 Remote Sensing*, vol. 29, no. 6, p. 807, Nov. 1991.
- 1758 [273] J. Friesen, H. C. Winsemius, R. Beck, K. Scipal, W. Wagner, and N. Van De Giesen, "Spatial and seasonal patterns of  
1759 diurnal differences in ERS Scatterometer soil moisture data in the Volta Basin, West Africa," *IAHS PUBLICATION*, vol.  
1760 316, p. 47, 2007.
- 1761 [274] K. C. McDonald, R. Zimmermann, and J. S. Kimball, "Diurnal and spatial variation of xylem dielectric constant in Norway  
1762 Spruce (*Picea abies* [L.] Karst.) as related to microclimate, xylem sap flow, and xylem chemistry," *IEEE Transactions on  
1763 Geoscience and Remote Sensing*, vol. 40, no. 9, pp. 2063–2082, Sep. 2002.
- 1764 [275] R. Torres, P. Snoeij, D. Geudtner, D. Bibby, M. Davidson, E. Attema, P. Potin, B. Rommen, N. Floury, M. Brown, I. N.  
1765 Traver, P. Deghaye, B. Duesmann, B. Rosich, N. Miranda, C. Bruno, M. L'Abbate, R. Croci, A. Pietropaolo, M. Huchler,  
1766 and F. Rostan, "GMES Sentinel-1 mission," *Remote Sensing of Environment*, vol. 120, pp. 9–24, May 2012.
- 1767 [276] A. A. Thompson, "Overview of the RADARSAT Constellation Mission," *Canadian Journal of Remote Sensing*, vol. 41,  
1768 no. 5, pp. 401–407, 2015.
- 1769 [277] "NASA Focused on Sentinel as Replacement for SMAP Radar," Nov. 2015. [Online]. Available:  
1770 <http://spacenews.com/nasa-focused-on-sentinel-as-replacement-for-smap-radar/>
- 1771 [278] S. C. M. Brown, S. Quegan, K. Morrison, J. C. Bennett, and G. Cookmartin, "High-resolution measurements of scattering  
1772 in wheat canopies-implications for crop parameter retrieval," *IEEE Transactions on Geoscience and Remote Sensing*,  
1773 vol. 41, no. 7, pp. 1602–1610, Jul. 2003.
- 1774 [279] H. Jörg, M. Pardini, I. Hajnsek, and K. P. Papathanassiou, "First multi-frequency investigation of SAR tomography  
1775 for vertical structure of agricultural crops," in *EUSAR 2014; 10th European Conference on Synthetic Aperture Radar;  
1776 Proceedings of. VDE*, 2014, pp. 1–4.
- 1777 [280] H. Joerg, M. Pardini, K. P. Papathanassiou, and I. Hajnsek, "Analysis of orientation effects of crop vegetation volumes by  
1778 means of SAR tomography at different frequencies," in *EUSAR 2016: 11th European Conference on Synthetic Aperture  
1779 Radar; Proceedings of. VDE*, 2016, pp. 1–4.

- 1780 [281] A. Reigber and A. Moreira, "First demonstration of airborne SAR tomography using multibaseline L-band data," *IEEE*  
1781 *Transactions on Geoscience and Remote Sensing*, vol. 38, no. 5, pp. 2142–2152, 2000.
- 1782 [282] M. Pardini, A. T. Caicoya, F. Kugler, S.-K. Lee, I. Hajnsek, and K. Papathanassiou, "On the estimation of forest  
1783 vertical structure from multibaseline polarimetric SAR data," in *2012 IEEE International Geoscience and Remote Sensing*  
1784 *Symposium*. IEEE, 2012, pp. 3443–3446.
- 1785 [283] E. Aguilera, M. Nannini, and A. Reigber, "Wavelet-based compressed sensing for sar tomography of forested areas,"  
1786 *IEEE Transactions on Geoscience and Remote Sensing*, vol. 51, no. 12, pp. 5283–5295, 2013.
- 1787 [284] J. D. Ballester-Berman, J. M. López-Sánchez, and J. Fortuny-Guasch, "Retrieval of biophysical parameters of agricultural  
1788 crops using polarimetric SAR interferometry," *IEEE Transactions on Geoscience and Remote Sensing*, vol. 43, no. 4, pp.  
1789 683–694, 2005.
- 1790 [285] J. D. Ballester-Berman, J. M. Lopez-Sanchez, and M.-J. Sanjuan, "Determination of scattering mechanisms inside rice  
1791 plants by means of PCT and high resolution radar imaging," in *2009 IEEE International Geoscience and Remote Sensing*  
1792 *Symposium*, vol. 5. IEEE, 2009, pp. V–138.
- 1793 [286] M. Pichierri, I. Hajnsek, and K. P. Papathanassiou, "A multibaseline Pol-InSAR inversion scheme for crop parameter  
1794 estimation at different frequencies," *IEEE Transactions on Geoscience and Remote Sensing*, vol. 54, no. 8, pp. 4952–  
1795 4970, 2016.
- 1796 [287] M. Pichierri and I. Hajnsek, "Comparing performances of crop height inversion schemes from multi-frequency Pol-InSAR  
1797 data," *IEEE Journal of Selected Topics in Applied Earth Observations and Remote Sensing*, vol. in review, 2016.
- 1798 [288] C. C. Chew, E. E. Small, K. M. Larson, and V. U. Zavorotny, "Vegetation sensing using GPS-interferometric reflectometry:  
1799 theoretical effects of canopy parameters on signal-to-noise ratio data," *IEEE Transactions on Geoscience and Remote*  
1800 *Sensing*, vol. 53, no. 5, pp. 2755–2764, 2015.
- 1801 [289] Q. Chen, D. Won, D. M. Akos, and E. E. Small, "Vegetation sensing using GPS Interferometric Reflectometry:  
1802 Experimental results with a horizontally polarized antenna," *IEEE Journal of Selected Topics in Applied Earth*  
1803 *Observations and Remote Sensing*, vol. PP, no. 99, pp. 1–10, 2016.
- 1804 [290] W. Wan, K. M. Larson, E. E. Small, C. C. Chew, and J. J. Braun, "Using geodetic GPS receivers to measure vegetation  
1805 water content," *GPS Solutions*, vol. 19, no. 2, pp. 237–248, 2015.
- 1806 [291] K. P. Hunt, J. J. Niemeier, L. K. da Cunha, and A. Kruger, "Using cellular network signal strength to monitor vegetation  
1807 characteristics," *IEEE Geoscience and Remote Sensing Letters*, vol. 8, no. 2, pp. 346–349, 2011.
- 1808 [292] G. Baroni and S. Oswald, "A scaling approach for the assessment of biomass changes and rainfall interception using  
1809 cosmic-ray neutron sensing," *Journal of Hydrology*, vol. 525, pp. 264–276, 2015.
- 1810 [293] T. E. Franz, M. Zreda, R. Rosolem, B. K. Hornbuckle, S. L. Irvin, H. Adams, T. E. Kolb, C. Zweck, and W. J. Shuttleworth,  
1811 "Ecosystem-scale measurements of biomass water using cosmic ray neutrons," *Geophysical Research Letters*, vol. 40,  
1812 no. 15, pp. 3929–3933, 2013.

1813  
1814  
1815  
1816  
1817  
1818  
1819  
1820

PLACE  
PHOTO  
HERE

**Susan Steele-Dunne** received the S.M. and Ph.D. degrees in hydrology from Massachusetts Institute of Technology, Cambridge, MA, USA, in 2002 and 2006, respectively. Since 2008, she has been with the Water Resources Section, Faculty of Civil Engineering and Geosciences, Delft University of Technology, Delft, The Netherlands. Her research interests include remote sensing, data assimilation, land atmosphere interactions, and land surface modeling. Dr. Steele-Dunne is a member of the American Meteorological Society and the American Geophysical Union. She has also served the American Geophysical Union Hydrology Section as a member of the Remote Sensing Technical Committee and the Hydrological Sciences Award Committee, and the American Meteorological Society as a member of the Hydrology Committee.

1821  
1822  
1823  
1824  
1825  
1826  
1827

PLACE  
PHOTO  
HERE

**Heather McNairn** received a Bachelor of Environmental Studies from the University of Waterloo, Waterloo, Canada, in 1987, a Masters in Soil Science from the University of Guelph, Guelph, Canada in 1991, and a Ph.D. in Geography from Universit Laval, Quebec City, Canada in 1999. Dr. McNairn is a senior scientist with Agriculture and Agri-food Canada. She has 25 years of experience researching methods to monitor crops and soil using multi-spectral, hyperspectral and Synthetic Aperture Radar (SAR) sensors. Dr. McNairn is an adjunct professor at the University of Manitoba (Winnipeg) and Carleton University (Ottawa).

1828  
1829  
1830  
1831  
1832  
1833  
1834  
1835  
1836  
1837  
1838

PLACE  
PHOTO  
HERE

**Alejandro Monsivais-Huerta** (S'06–M'07–SM'13) received the B.S. degree in telecommunications engineering from the National Autonomous University of Mexico, Mexico City, Mexico, in 2002 and the M.S. degree in microwaves and optical telecommunications and the Ph.D. degree in microwaves, electromagnetism, and optoelectronics from the University of Toulouse, Toulouse, France, in 2004 and 2007, respectively. From 2004 to 2006, he was with the Antennes, Dispositifs et Matériaux Microondes Laboratory, and from 2006 to 2007, with the Laboratoire d'Etudes et de Recherche en Imagerie Spatiale et Médicale, both at the University of Toulouse. From 2008 to 2009, he was as a Postdoctorate Research Associate at the Center for Remote Sensing, Department of Agricultural and Biological Engineering, University of Florida, Gainesville. Since 2010, he has been working as a researcher with the Superior School of Mechanical and Electrical Engineering campus Ticoman of the National Polytechnic Institute of Mexico, Mexico City. His research areas of interest are in microwave and millimeter-wave radar remote sensing, electromagnetic wave propagation, and retrieval algorithms.

1839  
1840  
1841  
1842  
1843  
1844  
1845  
1846  
1847

PLACE  
PHOTO  
HERE

**Jasmeet Judge** (S'94–M'00–SM'05) received the Ph.D. degree in electrical engineering and atmospheric, oceanic, and space sciences from the University of Michigan, Ann Arbor, MI, USA, in 1999. Currently, she is the Director of the Center for Remote Sensing and an Associate Professor in the Agricultural and Biological Engineering Department, Institute of Food and Agricultural Sciences, University of Florida, Gainesville, FL, USA. Her research interests include microwave remote sensing applications to terrestrial hydrology for dynamic vegetation; data assimilation; modeling of energy and moisture interactions at the land surface and in the vadose zone; and spatio-temporal scaling of remotely sensed observations in heterogenous landscapes. Dr. Judge is the Chair of the National Academies Committee on Radio Frequencies and a member of the Frequency Allocations in Remote Sensing Technical Committee in the IEEE-GRSS.

1848  
1849  
1850  
1851  
1852  
1853  
1854

PLACE  
PHOTO  
HERE

**Pang-Wei Liu** (S'09–M'13) received the PhD in Agricultural Engineering with a minor in Electrical Engineering from the University of Florida in 2013. He is currently a postdoctoral research associate at the Center for Remote Sensing in the Institute of Food and Agricultural Sciences, University of Florida. His research interests include modeling of active and passive microwave remote sensing for soil moisture and agricultural crops under dynamic hydrologic and vegetation conditions; data assimilation with crop growth models; application of LiDAR for forest biomass; and GNSS-R remote sensing for terrestrial applications. He is a member of the IEEE-GRSS and American Geophysical Union.

1855  
1856  
1857  
1858  
1859  
1860  
1861  
1862  
1863  
1864  
1865  
1866  
1867

PLACE  
PHOTO  
HERE

**Kostas Papathanassiou** (A'01–M'06–SM'09–F'13) received the Dipl.Ing. (Hons.) and Dr. (Hons.) degrees from the Graz University of Technology, Graz, Austria, in 1994 and 1999, respectively. From 1992 to 1994, he was with the Institute for Digital Image Processing (DIBAG), Joanneum Research, Graz. Between 1995 and 1999, he was with the Microwaves and Radar Institute, German Aerospace Center (DLR-HR), Wessling, Germany. From 1999 to 2000, he was a European Union Postdoctoral Fellow with Applied Electromagnetics, St. Andrews, U.K. Since October 2000, he has been a Senior Scientist with DLR-HR, leading the Information Retrieval Research Group. His main research interests are in polarimetric and interferometric processing and calibration techniques, polarimetric SAR interferometry, and the quantitative parameter estimation from SAR data, as well as in SAR mission design and SAR mission performance analysis. He was the recipient of the IEEE GRSS IGARSS Symposium Prize Award in 1998, the Best Paper Award of the European SAR Conference in 2002, the DLR Science Award in 2002, and the DLR Senior Scientist Award in 2011. He is a member of DLR's TanDEM-X and Tandem-L Science Teams, JAXA's ALOS-2 Cal-Val teams, ESA's BIOMASS mission Advisory Group, SAOCOM-SC Expert Team, JAXA's Carbon and Kyoto Initiative, and NASA's GEDI Mission Science Team.